Chromosomal resolution of a parasitic wasp genome reveals the colonisation of its symbiotic virus

SUPPLEMENTARY INFORMATION (NOTES, TABLES, FIGURES)

A. Global analyses

1. Genome sequencing and assembly

Supplementary Table 1. Sequencing and assembly statistics.

Statistics	*C. congregata*			*C. rubecula*	*C. glomerata*		*C. vestalis*	*C. flavipes*	*C. sesamiae*
Sequencing technology	454 single end	454 mate-pair (3,8, 20kb)	Illumina	Illumina	Illumina	PacBio	Illumina	Illumina	Illumina
Coverage	20 X	5 X	132 X	237 X	196 X	4 X	216 X	246 X	242 X
# Scaffolds	3,140			35,383	50,739		31,915	18 696	13,504
N50 scaffold	1,122.4 kb			12.8 kb	9.1 kb		14.6 kb	20.3 kb	26.6 kb
L50 scaffold count	48			4,490	6,813		2,549	2,071	1,699
Mean scaffold size	65,892			6,120	4,800		5,521	8,28	8,952
Median scaffold size	3,331			2,940	2,497		2,047	3,278	2,697
Longest scaffold	4,757 kb			156 kb	197 kb		561 kb	166 kb	228 kb
Total length	206.9 Mb			216.5 Mb	243.5 Mb		176.2 Mb	154.8 Mb	165.9 Mb
%N	6.68			3.97	4.62		3.75	1.78	2.74
GC content (%)	28.21			29.10	28.73		29.26	29.62	29.35

Supplementary Table 2. Statistics used for the genome size estimation (M: mean K-mer coverage, N: genome coverage, K: K-mer size, L: mean read length, N=(M*L)/(L-K+1)) and genome size measured by cytometry.

		C. congregata	*C. rubecula*	*C. glomerata*	*C. vestalis*	*C. flavipes*	*C. sesamiae*
k-mer counting estimation	M	149	160	106	156	176	171
	K	17	17	17	17	17	17
	L	98.94	91.07	79.32	91.55	98.84	98.77
	N	177.74	97.05	66.39	94.51	209.99	204.05
	Genome size estimation	215.9 Mb	204.7 Mb	160.8 Mb	129.8 Mb	178.1 Mb	193.2 Mb
	Genome assembled size	206.9 Mb	216.5 Mb	243.5 Mb	176.2 Mb	154.8 Mb	165.9 Mb
	Cytometry measure	n.a.	220 Mb	298 Mb	189 Mb	n.a.	n.a.

2. Chromosome scale assembly of *C. congregata* genome

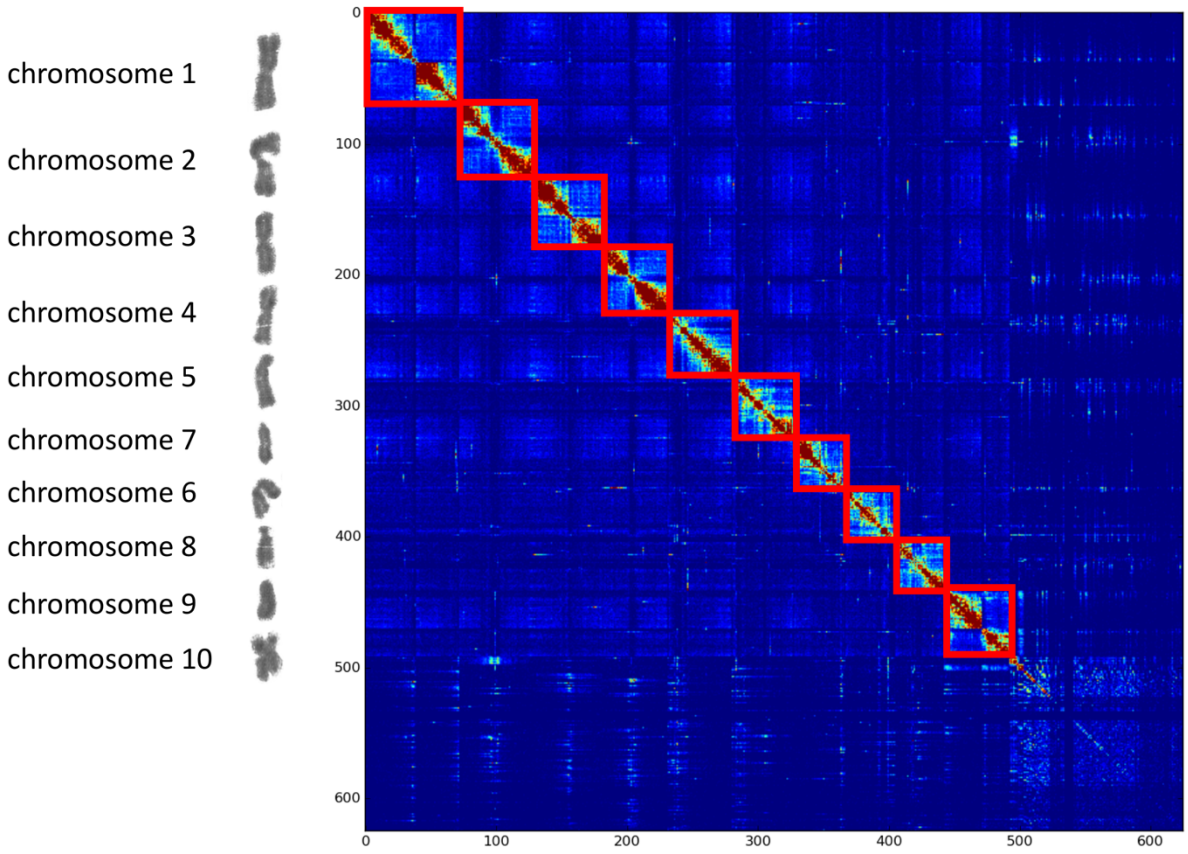

Supplementary Figure 1. Contact matrix between each fragment used for the GRAAL assembly, from blue the most distant to red the closest fragments. Along the two axis the fragments are organized according to this distance. The red frames have been added to visualize the chromosomes separations. The assignation of each chromosome has been performed using the chromosome length and centromere positions but also including sequences used for in situ hybridization performed by Belle and colleagues[1] (the chromosome pictures have been extracted from karyotype performed in this study).

Supplementary Table 3. Comparative statistics of *C. congregata* assembly strategies.

Statistics	*C. congregata* scaffolds	*C. congregata* chromosomes
# Scaffolds	3,140	1,790
N50 scaffold	1,122.4 kb	20,028.0 kb
L50 scaffold count	48	5
Mean scaffold size	65,892	111,241
Median scaffold size	3,331	1,708
Longest scaffold	4,757 kb	29,601 kb
Total length	206.9 Mb	199.1 Mb
%N	6.68	6.71
GC content (%)	28.21	27.97

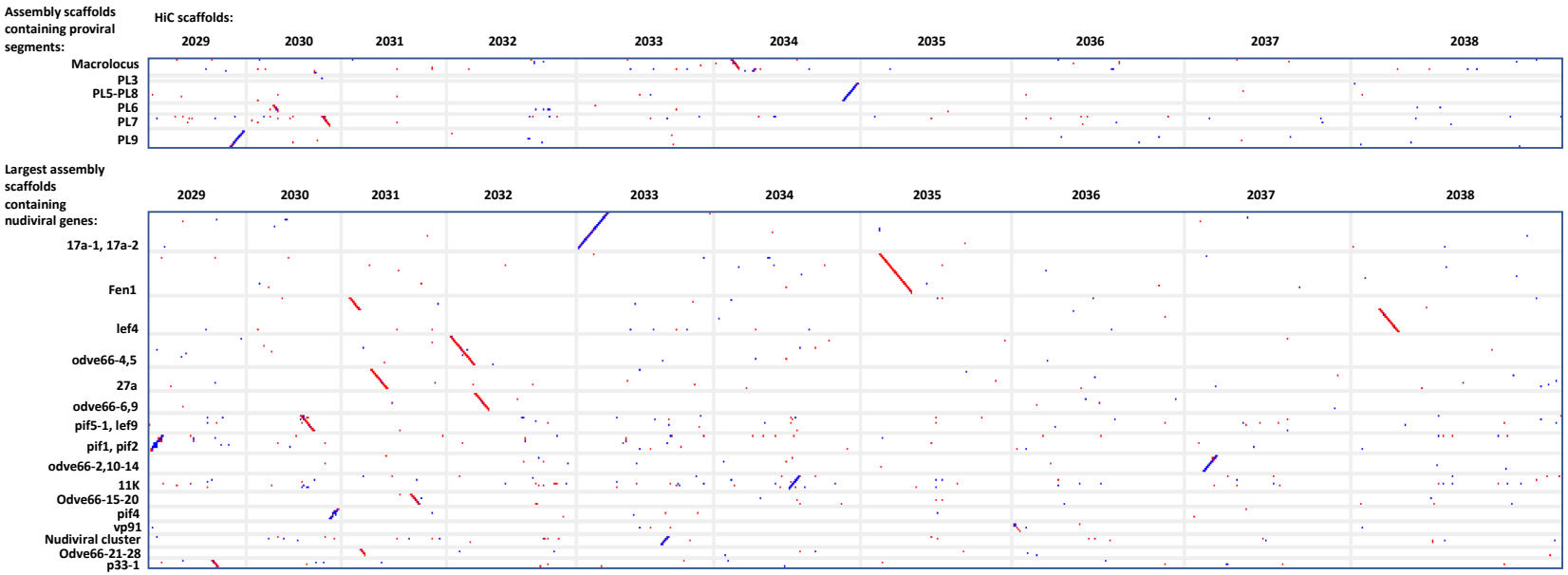

Supplementary Figure 2. Dot plot: assembly scaffolds/HiC scaffolds. Assembly scaffolds are confirmed by HiC scaffolds (except for the *lef4*-containing scaffold which is split in two pieces in HiC).

Supplementary Table 4. Chromosome size and centromere positions.

Chromosome	Chromosome size (bp)	Centromere start interval	Centromere stop interval	Centromere size [min - max]
C1	29,601,432	[12,811,254 - 13,152,523]	[13,793,916 - 14,111,909]	[641,393 - 1,300,655]
C2	23,655,861	[8,494,020 - 8,801,912]	[13,183,609 - 13,558,132]	[4,381,697 - 5,064,112]
C3	22,997,154	[8,843,013 - 9,160,875]	[12352173 - 12654164]	[3,191,298 - 3,811,151]
C4	20,820,356	[8,962,848 - 9,283,572]	[12,33,9695 - 12,649,662]	[3,056,123 - 3,686,814]
C5	20,027,981	[5,848,332 - 6,120,763]	[9,521,997 - 9,837,552]	[3,401,234 - 3,989,220]
C7	18,774,300	[13,936,098 - 14,262,658]	[16,606,145 - 16,890,888]	[2,343,487 - 2,954,790]
C6	17,819,366	[7,190,494 - 7,542,794]	[8,206,837 - 8,525,856]	[664,043 - 1,335,362]
C8	14,366,765	[8,317,315 - 8,636,383]	[9,295,605 - 9,620,272]	[659,222 - 1,302,957]
C9	13,378,970	[1,530,552 - 1,939,377]	[3,558,308 - 3,831,838]	[1,618,931 - 2,301,286]
C10	12,702,143	[3,965,924 - 4,320,652]	[6,170,807 - 6,462,798]	[1,850,155 - 2,496,874]

3. Genome annotations

Transposable elements

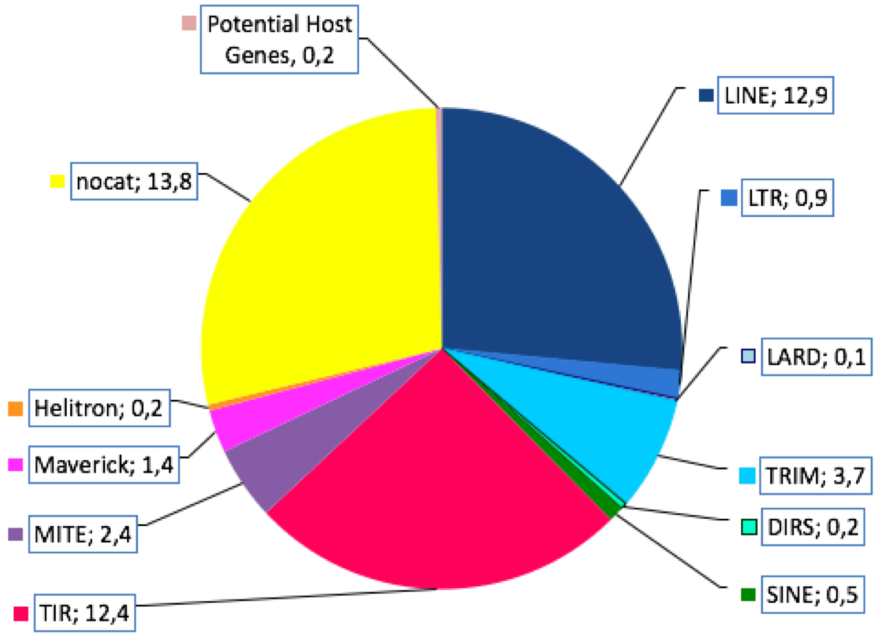

Supplementary Figure 3. Pie plot of transposable elements organized by families.

BV genes potentially originating from transposable elements

Analysis of the BV26 related sequences

The annotation of transposable elements by REPET revealed that the BV26 corresponded to a MITE (Miniature Inverted-repeat Transposable Element), 1606 bp long with 616 nt TIR (Terminal Inverted Repeats). A preliminary search detected 13 very similar copies of this sequence in the genome of *C. congregata*. The BV26 ORF presented no homology with TE proteins (blastx search against the RepBase protein database (RepBase20.05_REPET edition, https://www.girinst.org/) with default parameters.

Detection of longer related elements

We then used the 60 first nt of the TIR of this sequence in a blastn search against the genome of *C. congregata* and were able to detect and extract 197 sequences bordered by convergent TIRs (home-made script). Those sequences were blasted against the repbase protein database (RepBase20.05_REPET edition) (blastx, -evalue 1e-4). 49 sequences gave hits with TE proteins, among which 24 (46 different hits) had homology with Sola2 transposases (Class II elements[2]).

The presence of TIRs was rechecked on the sequences, with IRF[3]. We kept 146 sequences containing no N in the sequence, and the sequences were clustered using usearch v5.1 ([4] -id=0.8). Among the 31 clusters found, 6 of them, containing most of the sequences presenting homology with Sola2 elements and characterized by TIRs similar to the TIRs observed in BV26. Two other clusters corresponded to MITE sequences with no protein homology, but long TIRs, and containing amplified copies. This suggested that the MITE sequences could have derived of Sola2 elements after internal deletions. These 8 clusters corresponded to 82 sequences and were kept for further analyses (Supplementary Figure 4 A). Other clusters, presenting either terminal sequences not corresponding to the BV26 TIRs (internal parts of TIRs of another TE family), or sequences of various sizes that may correspond to relics having inserted foreign sequences, were excluded from the analyses. The presence of a large number of sequences varying in size, suggest that this element is ancient.

Characterization of insertions sites

In order to better characterize this element, the flanking sequences of the selected copies (200 nt each side) were used in a blastn search against the *C. congregata* genomes to detect paralogous (repetitive) sequences without Sola2 insertions. Comparison of these paralogous sequences with Sola2 corresponding insertion sites allowed us to propose that the TIRs of the elements start with 4 Gs, and that the element inserts into TA-rich sequences, creating a 4-bp target site duplication as expected for Sola2 elements[2]. For a number of cases, insertion sites occurred in very TA-rich microsatellites-like TA sequences and the paralogous sites displayed a variability in the number of TA repeats, making the TSD difficult to identify with confidence. Some examples of clear-cut cases are shown in Supplementary Figure 4 B.

Characterization of Sola2 sequences

The 46 sequence fragments presenting homology to Sola2 transposases were translated (and merged when corresponding to different fragment of the same copy) and aligned with selected sequences of Sola2 from RepBase, plus 3 sequences of the related Sola3 element used as outgroup (MAFFT v7[5]) The alignment was truncated to keep only the 250 AA-long best conserved part (AA 240 to 520 of Sola2-1_Nvi) for a phylogenetic analysis using FastTree[6] 2 sequences were removed (deleted over this conserved region). The resulting tree suggests a monophyletic origin of the *C. congregata* Sola2 sequences. Our knowledge of Sola2 elements remains fragmentary, only few genomes having been screened. Closest sequences in Repbase are found in the related parasitoid

Nasonia vitripennis, and two ant species (Supplementary Figure 4 C). Potentially active sequences (long ORFs, not stop codons or frameshift, with one intron) could be identified in clusters 6 and 16.

Distribution among other genomes

Finally, we searched for related sequences in 5 other *Cotesia* species and in other genomic sequences from Hymenoptera and Lepidoptera. For this, coding fragments from one sequence per cluster were blasted (blastn, -evalue 1e-10) against the genome assemblies of these two insect orders, available in NCBI (by October 14th, 2019), representing 309 assemblies of Hymenoptera (278 species) and 204 assemblies of Lepidoptera (64 species). Hits representing the same sequence were merged using a home-made script (maximum distance for merging 2 hits: 2000 nt, and minimum final size: 100 nt). The distribution of the elements among the different species tested, as well as the distribution of the hits among the different assemblies for each superfamily of organisms is shown on Supplementary Figure 4. Phylogenetic relationships between taxa are derived from[7,8]. Among Hymenoptera, similar sequences were detected in 71 species, mostly within the Parasitoida superfamily, with some species displaying a high number of sequences (in Chalcidoidea and Ichneumonoidea), as well as in some other groups, especially in ants (Formicoidea). 17 Lepidoptera species also exhibited some related sequences, but always in relatively low copy numbers. We computed the percentage of identity given by the blastn search, between those hits and the *C. congregata* query sequences (Supplementary Figure 4 E). The most abundant cluster in *Cotesia* was Cluster 7 (See Supplementary Table 5). For this cluster, the average percentages of identity were higher for *Cotesia* genomes than for other Hymenoptera or for Lepidoptera. However, sequences in Lepidoptera had a higher identity than Hymenoptera sequences. The best Lepidoptera hits (>90% over 300 nt) were found in *Papillio machaon*. This may reflect some past events of horizontal transfers between these two orders of insects[9]. Other clusters presented contrasted patterns suggesting absence of close sequences in some *Cotesia* genomes, and/or existence of other Sola2 cluster not found in *C. congregata*.

Distribution of other repeated sequences associated to BV genes

The same blastn procedure was applied to all the consensus sequences corresponding to repetitive sequences. The number of hits is shown for each consensus on Supplementary Table 5.

Supplementary Table 5. Distribution of reconstituted hits for different repeated sequences related to expressed BV genes.

	Sola2 ORF (BV26)						MITE BV26		REPET consensus sequences								
	Cluster 6	Cluster 7	Cluster 8	Cluster 15	Cluster 16	Cluster 20	Cluster 18	Cluster 23	BV14.3	BV2.3	BV21.1	BV26	BV3.5	BV3.7	BV30.5B	BV4.4	BV7
Cotesia congregata	23	70	10	3	11	13	231	548	256	37	100	717	224	108	53	313	889
Cotesia rubecola	17	130	64	12	9	9	297	342	365	24	80	516	145	102	117	479	539
Cotesia glomerata	10	112	36	15	4	9	192	396	238	30	69	502	225	117	148	469	533
Cotesia vestalis	20	74	26	15	8	9	106	255	137	5	32	345	87	32	52	161	419
Cotesia sesamiae	23	77	30	4	7	4	109	424	122	3	39	486	106	20	68	213	479
Cotesia flavipes	25	79	43	9	6	5	142	369	98	2	36	476	123	20	43	251	480
Hymenoptera (w/o *Cotesia*)	523	1074	247	747	453	171	156	674	332	19	65	190	190	81		325	
Lepidoptera	2	9	1	10	15	1	32	147									
	643	1625	457	815	513	221	1265	3155	1548	120	421	3232	1100	480	481	2211	3339

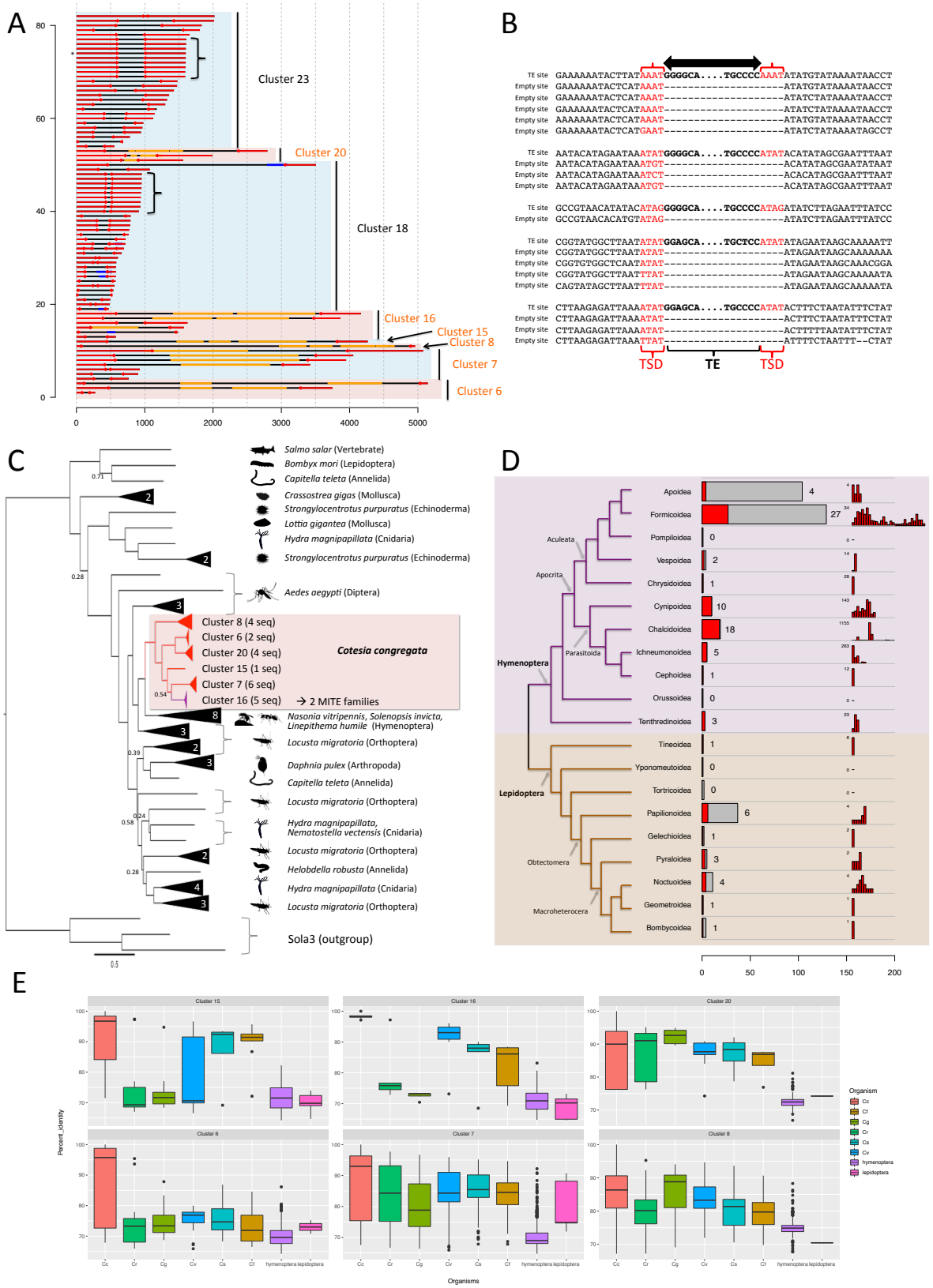
A
Cluster 23
Cluster 20
Cluster 18
Cluster 16
Cluster 15
Cluster 8
Cluster 7
Cluster 6
B
TE site
Empty site
TSD
TE
TSD
C
Salmo salar (Vertebrate)
Bombyx mori (Lepidoptera)
Capitella teleta (Annelida)
Crassostrea gigas (Mollusca)
Strongylocentrotus purpuratus (Echinoderma)
Lottia gigantea (Mollusca)
Hydra magnipapillata (Cnidaria)
Strongylocentrotus purpuratus (Echinoderma)
Aedes aegypti (Diptera)
Cluster 8 (4 seq)
Cluster 6 (2 seq)
Cluster 20 (4 seq)
Cluster 15 (1 seq)
Cluster 7 (6 seq)
Cluster 16 (5 seq)
Cotesia congregata
→ 2 MITE families
Nasonia vitripennis, Solenopsis invicta, Linepithema humile (Hymenoptera)
Locusta migratoria (Orthoptera)
Daphnia pulex (Arthropoda)
Capitella teleta (Annelida)
Locusta migratoria (Orthoptera)
Hydra magnipapillata, Nematostella vectensis (Cnidaria)
Locusta migratoria (Orthoptera)
Helobdella robusta (Annelida)
Hydra magnipapillata (Cnidaria)
Locusta migratoria (Orthoptera)
Sola3 (outgroup)
D
Hymenoptera
Aculeata
Apocrita
Parasitoida
Apoidea
Formicoidea
Pompiloidea
Vespoidea
Chrysidoidea
Cynipoidea
Chalcidoidea
Ichneumonoidea
Cephoidea
Orussoidea
Tenthredinoidea
Lepidoptera
Obtectomera
Macroheterocera
Tineoidea
Yponomeutoidea
Tortricoidea
Papilionoidea
Gelechioidea
Pyraloidea
Noctuoidea
Geometroidea
Bombycoidea
E
Cluster 15
Cluster 16
Cluster 20
Cluster 6
Cluster 7
Cluster 8
Percent_identity
Organisms
Organism
Cc
Cf
Cg
Cr
Cs
Cv
hymenoptera
lepidoptera

Supplementary Figure 4. Characteristics of Sola2 elements from *C. congregata.* **A** Structure of the 82 sequences belonging to the 8 main clusters. The x-axis is the length in nt. Six clusters (orange) contained sequences with homology to Sola2 transposase (orange part). Blue parts indicate homology with other TEs from RepBase. The two more abundant correspond to 2 MITE clusters and copies resulting from amplification (same size and sequences) are highlighted by brackets. Red arrows represent the TIRs of the elements. The asterisk indicates the initial copy corresponding to BV26. **B** Graph showing the target site duplication (4-nt, TA rich) deduced from the comparison of some Sola2 insertions sites with paralogous empty sites. As for typical Sola2 element, TIRs start by G-rich sequences. **C** Phylogenetic tree showing the relationships between Sola2 translated sequences from *C. congregata* (framed branches) and other Sola2 transposases from RepBase. Black triangles group TE consensus sequences from the same species (number of sequences is indicated). Open triangles represent consensus sequences of Sola3 elements (RepBase) used as an outgroup. Numbers on the branches are the robustness (local bootstraps) as implemented in FastTree. One group (purple) may be at the origin of the 2 MITEs families (based on TIR similarities). **D** Distribution of related Sola2 elements in genomes of hymenoptera and lepidoptera, available in NCBI. Grey bars represent the number of species for which genome sequences are available, and tested for the presence of Sola2 sequences. The red parts of the bars correspond to the number of species in which blastn hits have been found (numbers of species are indicated on the right of the bars. The number of different hits for each genome assembly is shown at the far right, the numbers beside correspond to the maximum number of hits found in one assembly (the highest bar in each barplot). Note that the number of assemblies can exceed the number of positive species (several genome assemblies for one species). **E** Boxplots showing the distribution of the percentage of identity between the *C. congregata* Sola2 sequences (ORF) (1 copy per cluster) and the blastn hits found in the various genomes. Cc: *C. congregata*, Cr: *C. rubecula*, Cg: *C. glomerata*, Cv: *C. vestalis*, Cs: *C. sesamiae*, Cf: *C. flavipes.*

Supplementary Table 6. Databases used during the annotation process.

	Species	Version	Database	Link
Automated annotation	*Apis mellifera*	v3.2	Beebase	http://hymenopteragenome.org/beebase/
	Nasonia vitripennis	v1.2	NasoniaBase	http://www.hymenopteragenome.org/nasonia/
	Acromyrmex echinatior	v.3.8	AntGenomes	http://antgenomes.org/
	Atta cephalotes	v1.0	AntGenomes	http://antgenomes.org/
	Camponotus floridanus	v1.0	AntGenomes	http://antgenomes.org/
	Harpegnathos saltator	v1.0	AntGenomes	http://antgenomes.org/
	Linepithema humile	v1.2	AntGenomes	http://antgenomes.org/
	Pogonomyrmex barbatus	v1.2	AntGenomes	http://antgenomes.org/
	Solenopsis invicta	v2.2.3	AntGenomes	http://antgenomes.org/
Functional annotation	*Acromyrmex echinatior*	v.3.8	AntGenomes	http://antgenomes.org/
	Apis mellifera	v3.2	Beebase	http://hymenopteragenome.org/beebase/
	Drosophila melanogaster	v6.03	Flybase	http://flybase.org/
	Nasonia vitripennis	v1.2	NasoniaBase	http://www.hymenopteragenome.org/nasonia/
	Manduca sexta	OGS 2.0_20140407	ManducaBase	http://agripestbase.org/manduca

Supplementary Table 7. Genome annotation statistics

Statistics	*C. congregata*	*C. rubecula*	*C. glomerata*	*C. vestalis*	*C. flavipes*	*C. sesamiae*
Number of predicted genes	14,140	22,795	23,498	19,239	17,381	17,785
Mean gene size (bp)	5,919.47	2,852.67	2,669.74	2,840.57	3,238.76	3,466.08
Number of exons	69,667	96,948	95,98	84,368	85,318	88,955
Mean number of exon by gene	4.93	4.25	4.08	4.39	4.91	5.00
Mean exon size (bp)	365.33	310.30	304.81	306.69	306.74	313.94
% coding sequence in genome	12.30	13.89	12.01	14.69	16.90	16.83
Number of gene without intron	1630	2815	2919	2330	1803	1687
Mean intron size (bp)	1047.62	469.23	459.88	439.81	441.39	471.76

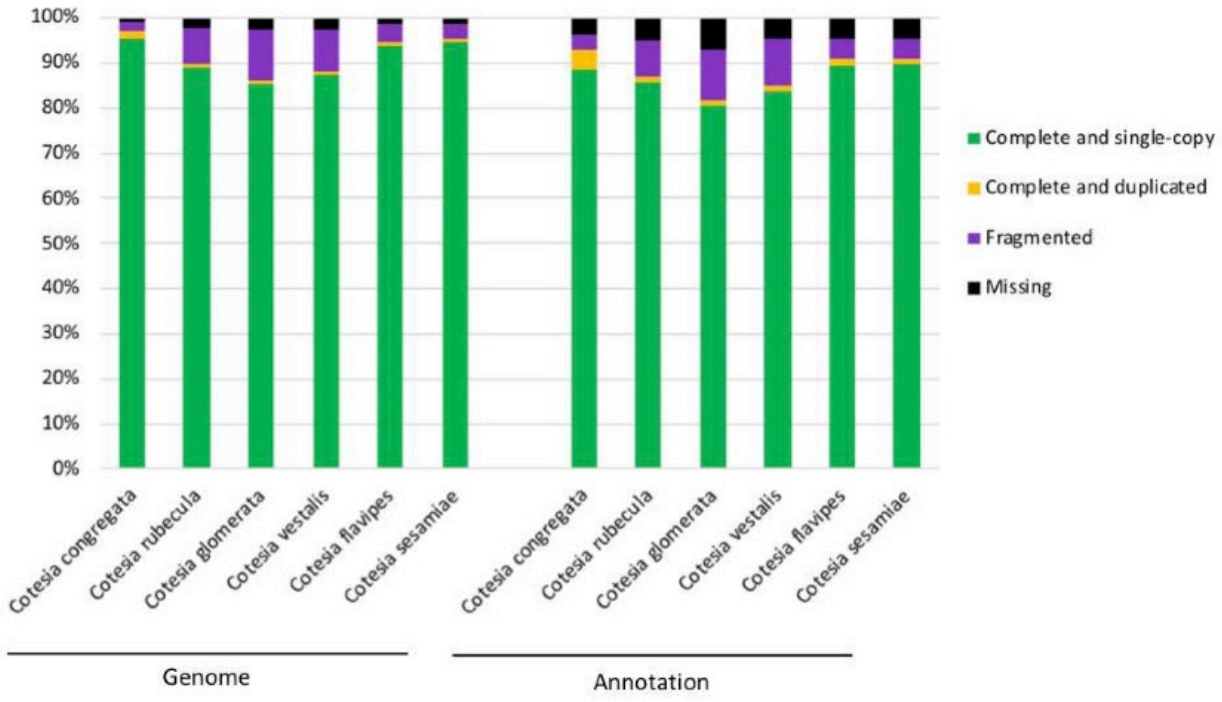

Supplementary Figure 5. BUSCO results obtained on genome and annotation of each *Cotesia* species.

4. RNA-Seq analyses

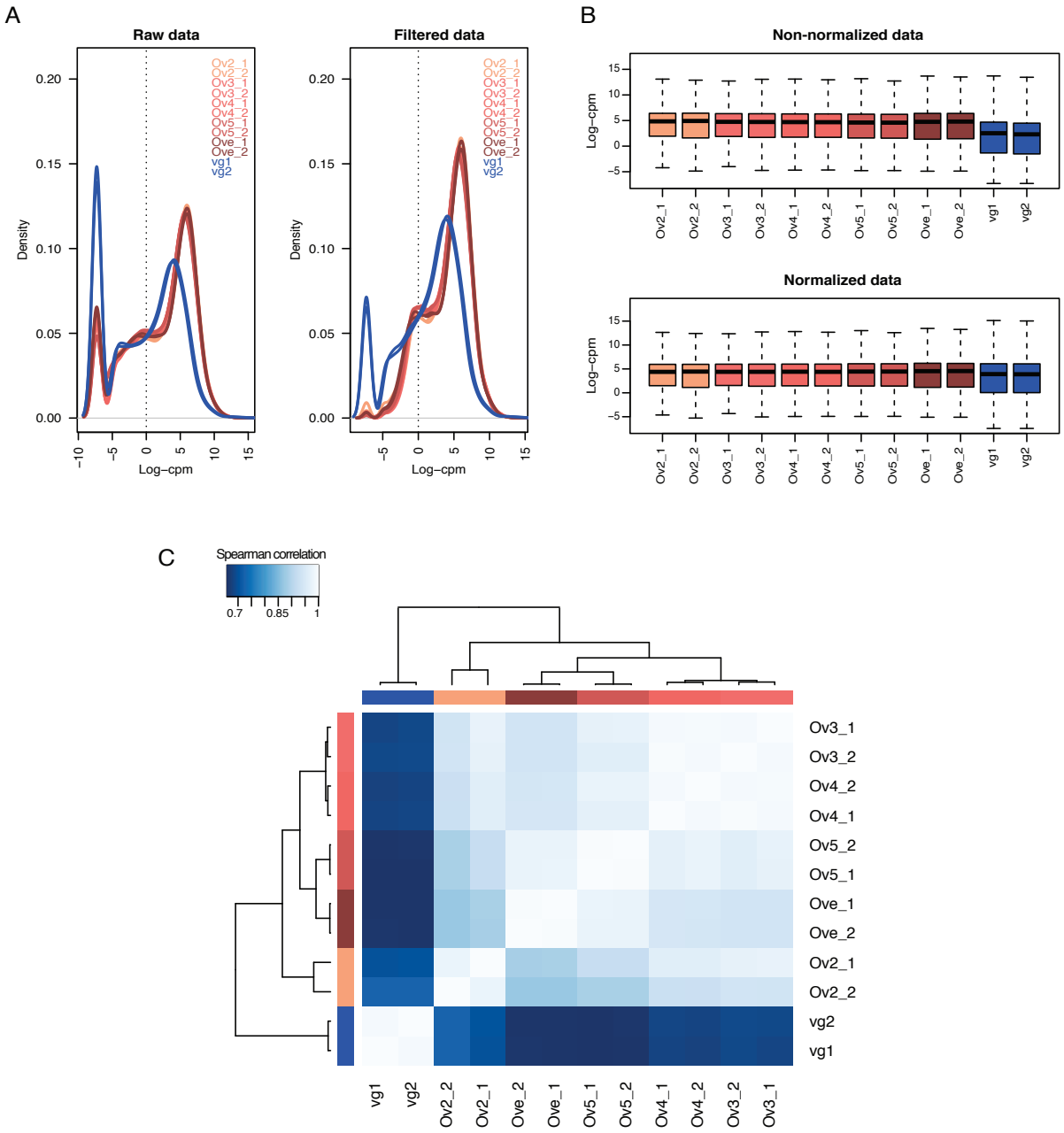

Supplementary Figure 6. Gene expression analysis of ovaries and venom glands of *Cotesia congregata.* **A.** Density plots representing expression levels of all expressed genes (Raw data: 13,607 genes) and after filtering the genes that do not show CPM > 0.4 in at least 2 libraries on the 12 analyzed libraries (Filtered data: 11,216 genes). **B.** Expression level distribution of the genes (filtered data) before and after CPM normalization using TMM method in edgeR. **C.** Heatmap of Spearman correlation between the 12 analyzed libraries. The unsupervised clustering did not reveal discrepancies between biological replicates, then all libraries were retained for further analyses. Ov2, Ov3, Ov4 and Ov5 represent ovary samples collected at different larval stages. Ove and vg respectively refer to ovaries and venom glands from adult wasp.

B. Phylogenetic considerations

Monophyly of the bracovirus-bearing lineage

Bracoviruses have so far been identified from the Microgastrinae (many species), Cardiochilinae (especially *Toxoneuron nigriceps*), Miracinae, Mendesellinae[10] and Cheloninae (several genera, but especially *Chelonus inanitus*). These all belong to what is commonly referred to today as the "microgastroid assemblage". To date, no sample from this group of subfamilies has ever failed to reveal an associate bracovirus (although of course the sampling is still rather sparse). A grouping within the braconid wasps very roughly corresponding to this assemblage, as currently conceived, has been recognized since at least the 1960's, if not before, although its current composition was not well understood (and to some extent is still not fully supported by strong evidence for a few possibly peripheral taxa). A close relationship between Microgastrinae, Cardiochilinae and Miracinae (sometimes also Adeliinae) was clear, but it was not until later studies showed that Adeliinae actually belong within the Cheloninae[11,12] and two new related subfamilies, the South African Khoikhoiinae[13] and the largely Neotropical Mendesellinae[14] were described, that the core microgastroid taxa were identified. Quicke and Van Achterberg[15], in a morphology-based phylogenetic study of Braconidae, found Dirrhopinae and Ichneutinae, both suspected relatives, to be part of the same assemblage, but as its earliest-diverged lineages. To date neither Dirrhopinae nor Ichneutinae (both relatively uncommon groups) have been surveyed for bracoviruses.

Monophyly of the bracovirus-bearing lineage of braconid wasps was first established using morphological and molecular data by[16] and subsequently confirmed by a number of molecular phylogenetic studies (e. g.[17-21]. The (presumably single) origin of the bracoviruses in these wasp groups has been confirmed as from ancestral nudiviruses[10], whose association with insects extends back much earlier[22].

Relationships among microgastroid subfamilies

Initially, relationships among the microgastroid subfamilies were established primarily using morphological data[14]. As additional subfamilies in the assemblage were described, and

molecular data became available[16,17,20,21], the relationships shown in Figure 1 began to be confirmed. There still remains some uncertainty about the exact relationships among the subfamilies, and about the relationship of Ichneutinae and Dirrhopinae to the core microgastroids, but generally speaking this is one of the best-established groupings within the braconid wasps. One constant is that Cheloninae (including Adeliini) is likely to be sister to the clade including Mendesellinae, Khoikhoiinae, Cardiochilinae, Miracinae and Microgastrinae, diverging from the others roughly 100 million years ago.

Relationships within Microgastrinae

The subfamily Microgastrinae is one of the most species-rich parasitoid groups on earth, with an estimated fauna of 17-46,000 species worldwide, based on various field-study extrapolations from the described species. Genus level systematics of the group remains in flux – currently 81 genera are recognized[23], several of them containing more than 1,000 species. As a result of this diversity, and also due to the genera having apparently evolved in a rapid burst roughly 50 million years ago[19,20,24,25], the higher-level phylogeny within the subfamily based on molecular and morphological data remains relatively poorly understood. Nevertheless, several relatively well-established relationships relevant to comparative bracovirus genomics are clear: a very close relationship between Cotesia Cameron and Glyptapanteles Ashmead, a cluster of related genera centered around Apanteles Foerster, and a relatively early divergence between Microplitis Foerster and its close relatives, and the other genera. Thus, we would expect the bracoviruses of Cotesia and Glyptapanteles to be relatively similar, and those of Microplitis to be among the most distant among the Microgastrinae.

C. Bracovirus

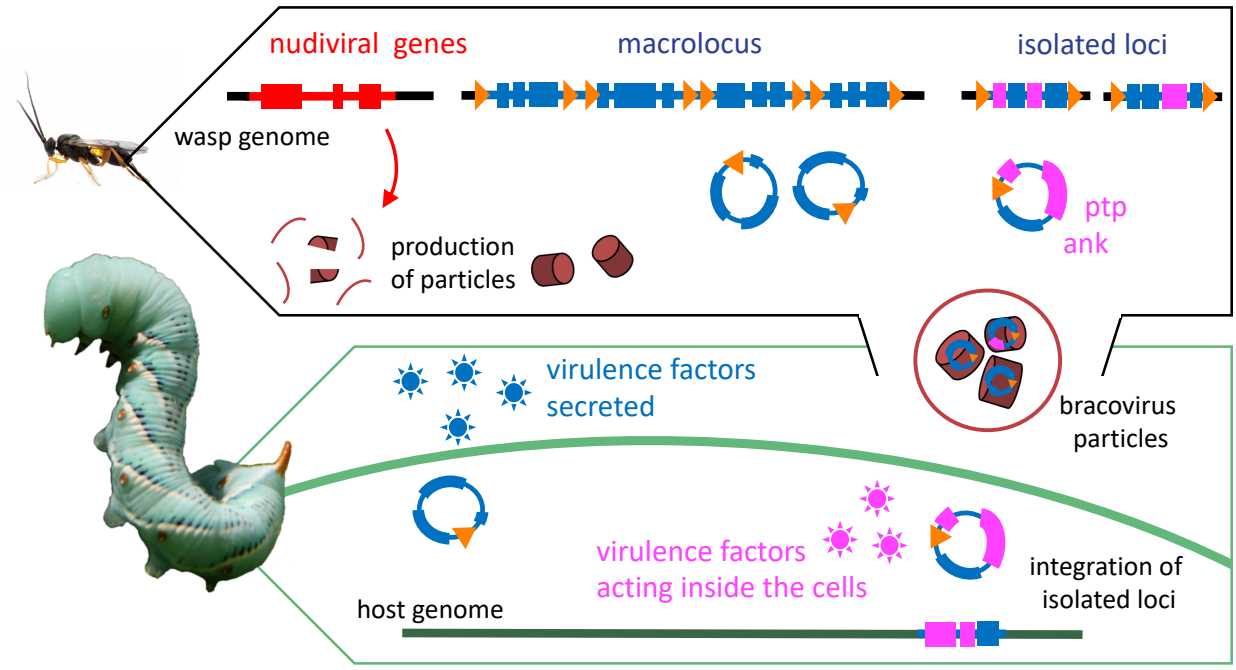

Supplementary Figure 7. Schematic representation of the bracovirus production in wasp ovaries and their function in host cells. Circles from isolated loci, encoding in particular *ptp* and *Vank* genes, integrate into parasitized host DNA using HIM site mediated mechanism.

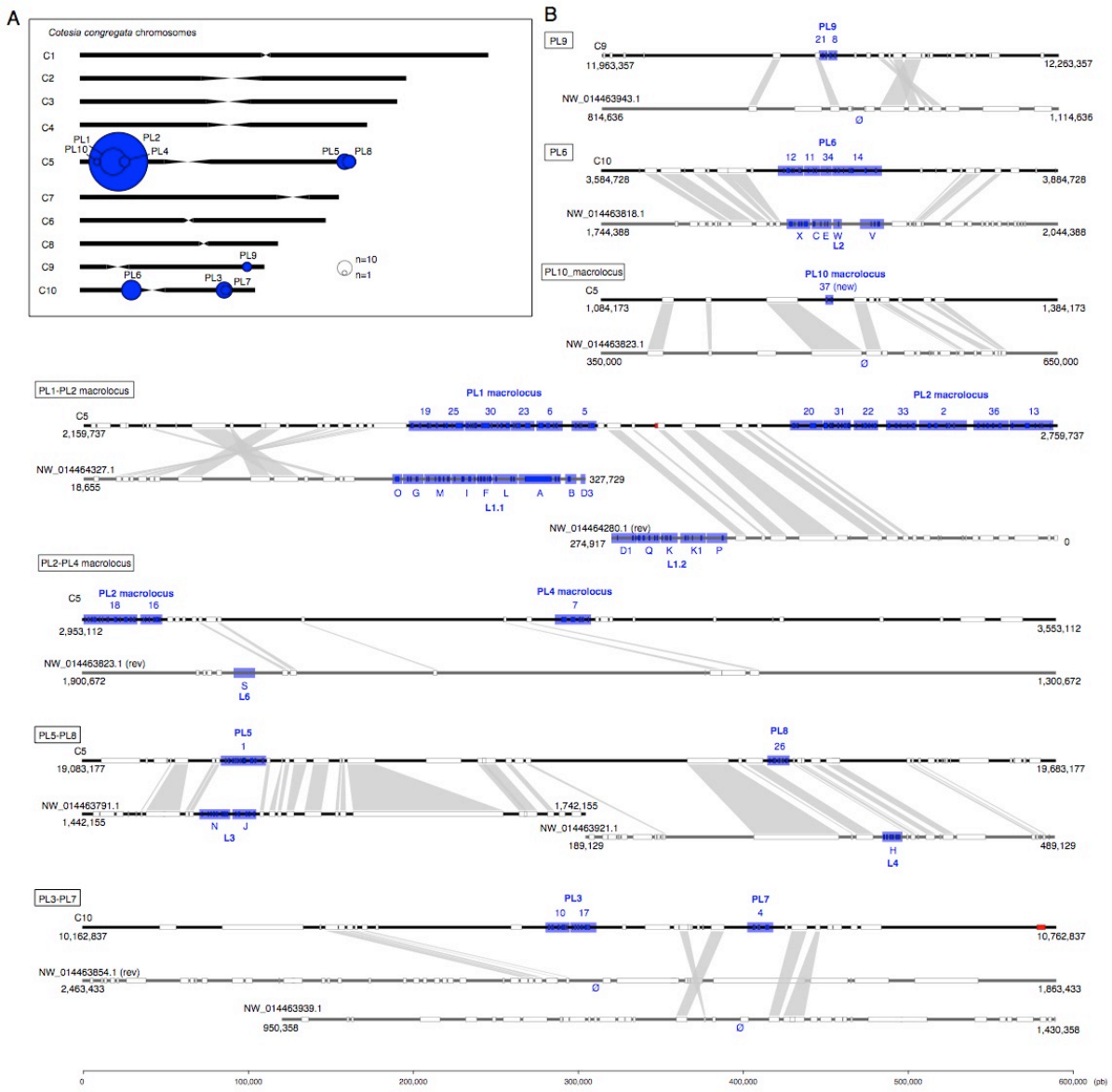

Supplementary Figure 8. Synteny between Proviral Loci (PL) of *C. congregata*_and *M. demolitor*. **A** *C. congregata* chromosomes map. **B** Comparison of *C. congregata* and *M. demolitor* *proviral loci*. *C. congregata* chromosomes and *M. demolitor* genome scaffolds are represented in black and dark grey respectively. Numbers 1 to 37 correspond to the 37 segments identified in *C. congregata* with the corresponding proviral loci indicating above and identified in *C. congregata* chromosomes map. Blue boxes indicate virulence genes while white boxes refer to non-virulence genes. *M. demolitor* scaffolds for which the orientation if reversed compared to *C. congregata* chromosomes are indicated by "rev". The scale shows length in bp. Ø indicates the absence of orthologous segment in *M. demolitor* genome.

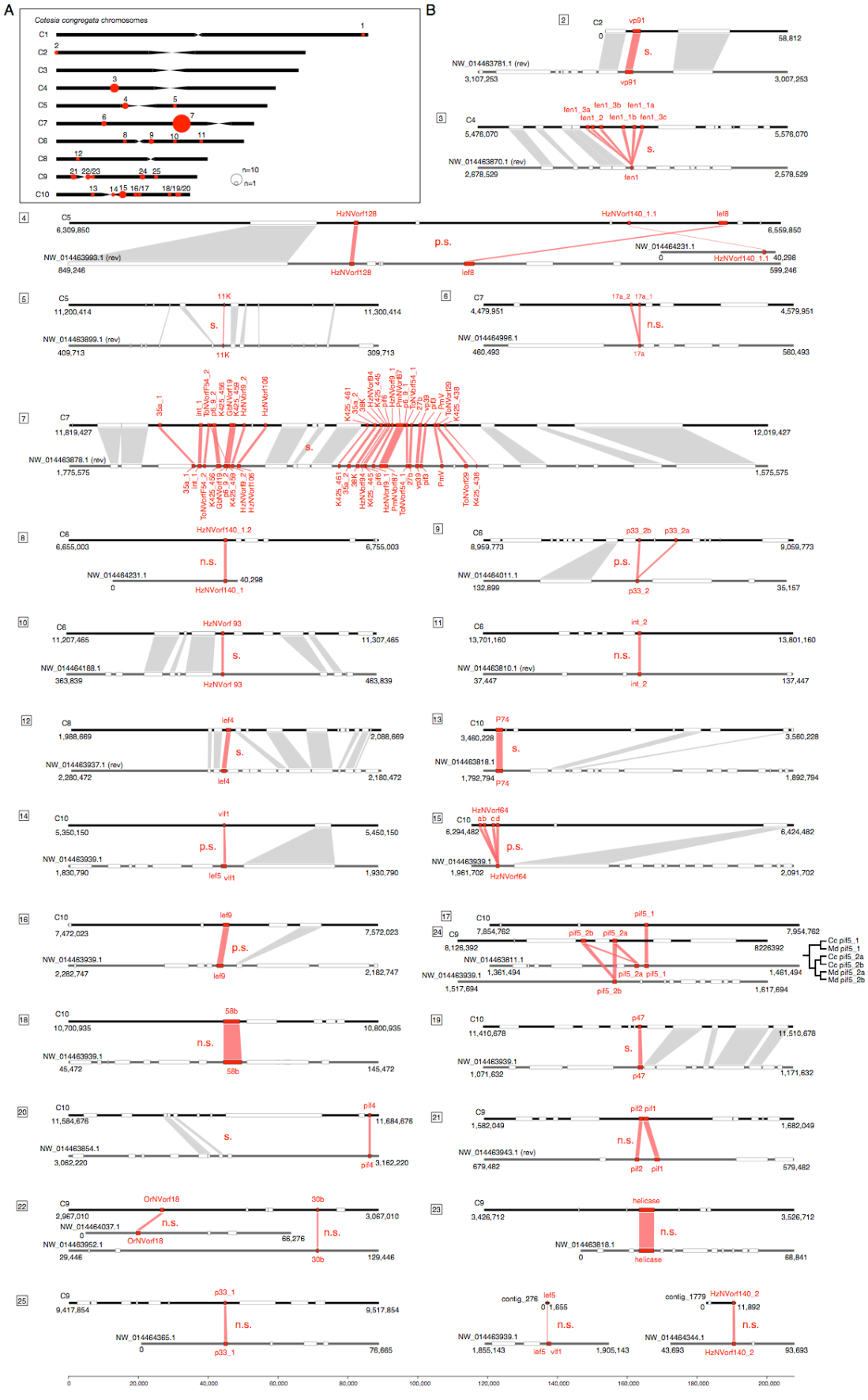
A
Cotesia congregata chromosomes
C1
C2
C3
C4
C5
C7
C6
C8
C9
C10
n=10
n=1
B
vp91
NW_014463781.1 (rev)
fen1
NW_014463870.1 (rev)
HzNVorf128
lef8
NW_014463993.1 (rev)
NW_014464231.1
HzNVorf140_1.1
11K
NW_014463899.1 (rev)
t7a
NW_014464996.1
NW_014463878.1 (rev)
HzNVorf140_1.2
NW_014464231.1
HzNVorf140_1
p33_2
NW_014464011.1
HzNVorf 93
NW_014464188.1
int_2
NW_014463810.1 (rev)
lef4
NW_014463937.1 (rev)
P74
NW_014463818.1
vlf1
lef5
NW_014463939.1
HzNVorf64
pif5_1
pif5_2b
pif5_2a
NW_014463811.1
58b
p47
pif4
NW_014463854.1
pif2
pif1
NW_014463943.1 (rev)
OrNVorf18
30b
NW_014464037.1
NW_014463952.1
helicase
p33_1
NW_014464365.1
contig_276
contig_1779
HzNVorf140_2
NW_014464344.1
n.s.
p.s.
s.

Supplementary Figure 9. Synteny between nudiral genes containing regions of *C. congregata* and *M. demolitor*. **A** *C. congregata* chromosomes map. **B** Comparison of nudiviral genes regions of *C. congregata* and *M. demolitor*. To validate a synteny between the two specie (indicated by "s." for synteny), we searched for at least two hymenopteran (non-viral) orthologous gene in the vicinity of homologous nudiviral gene(s) of the two species. If only one non-nudiviral orthologous gene was present we considered synteny as probable ("p.s.": probable synteny). Finally, when no orthologous gene was present in the vicinity of the nudiviral gene(s) in the two species, we considered the regions containing nudiviral genes were not homologous ("n.s": no synteny). *C. congregata* chromosomes and *M. demolitor* genome scaffolds are represented in black and dark grey respectively. Numbers 1 to 26 correspond to the 26 nudiviral loci identified in *C. congregata* chromosomes map. Red boxes indicate nudiviral genes and white boxes refer to hymenopteran genes. *M. demolitor* scaffolds for which the orientation is reversed compared to *C. congregata* chromosomes are indicated by "rev". The scale shows length in bp.

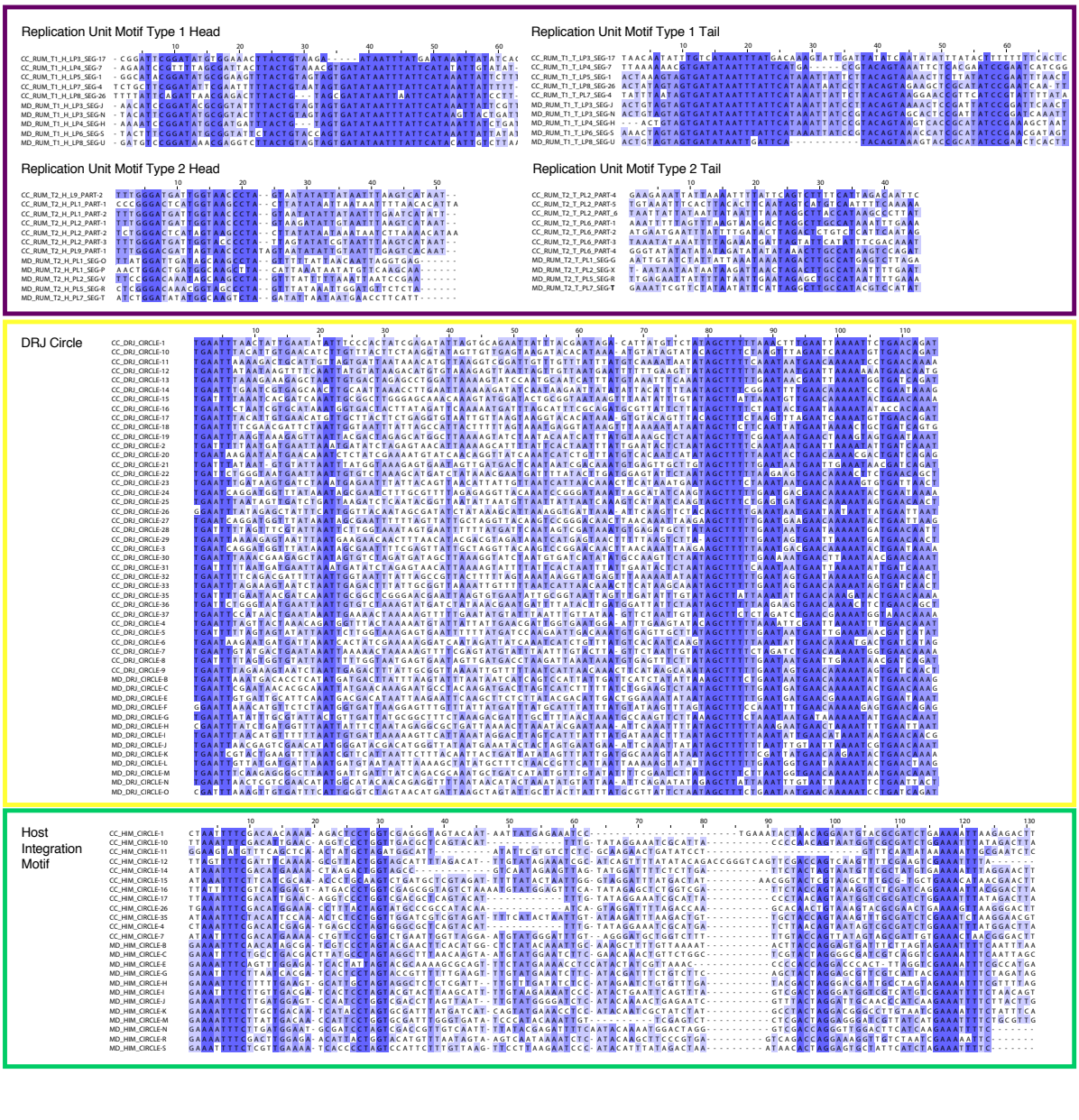

Supplementary Figure 10. In purple framework, the alignment of Replication Unit Motifs (RUM) including *C. congregata* and *M. demolitor* sequences. In yellow framework, the alignment of the circle Direct Repeat Junctions (DRJ). In green framework, the alignment of the Host Integration Motifs (HIM).

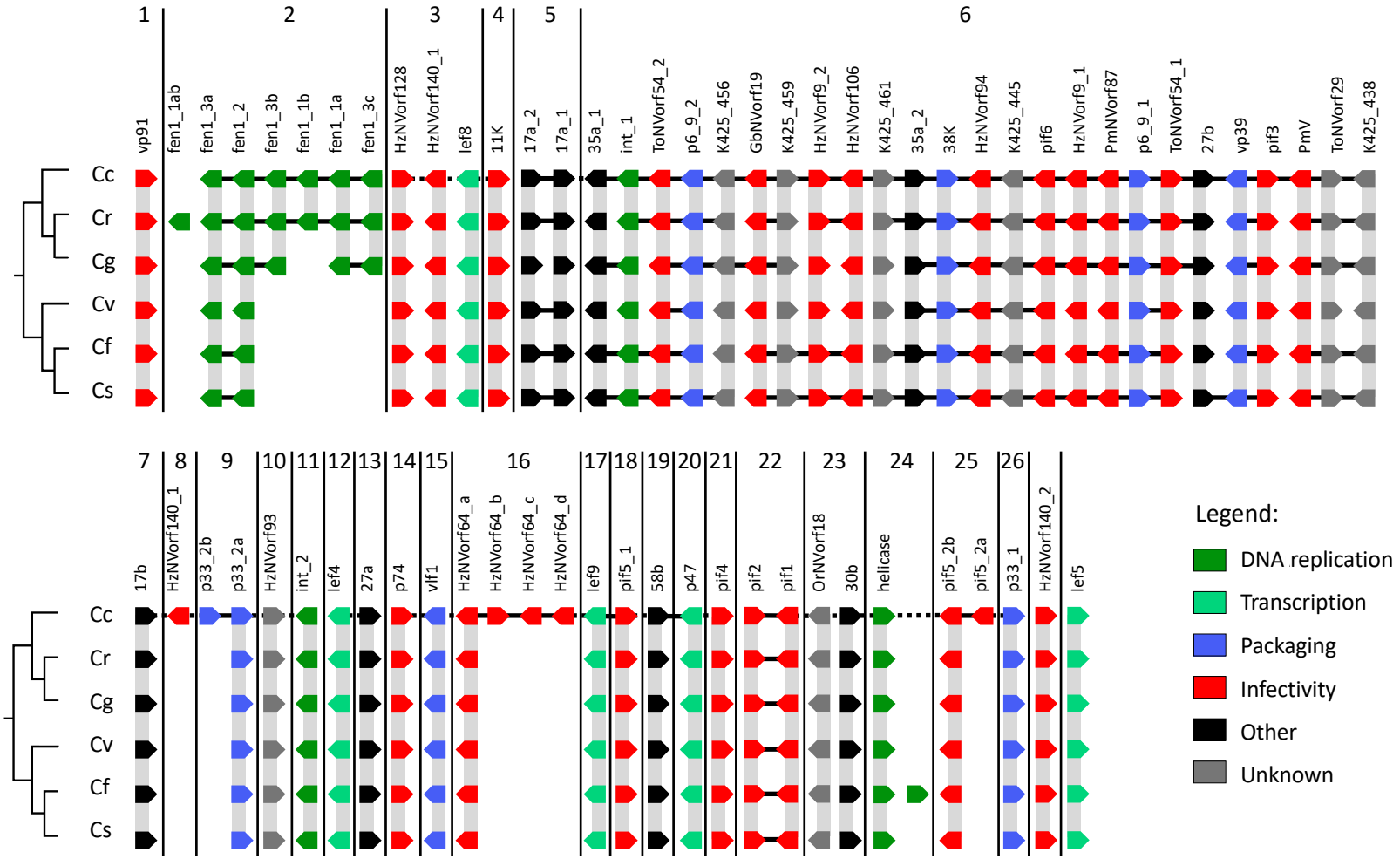

Supplementary Figure 11. Synteny of nudiviral genes across *Cotesia* species. Continuous black lines represent scaffolds and arrows indicate the orientation of the genes in each species. Number 1 to 26 correspond to the 26 nudiviral loci identified in *C. congregata* chromosomes. Cc, Cr, Cg, Cv, Cf, and Cs refer respectively to *C. congregata*, *C. rubecula*, *C. glomerata*, *C. vestalis*, *C. flavipes*, and *C. sesamiae*.

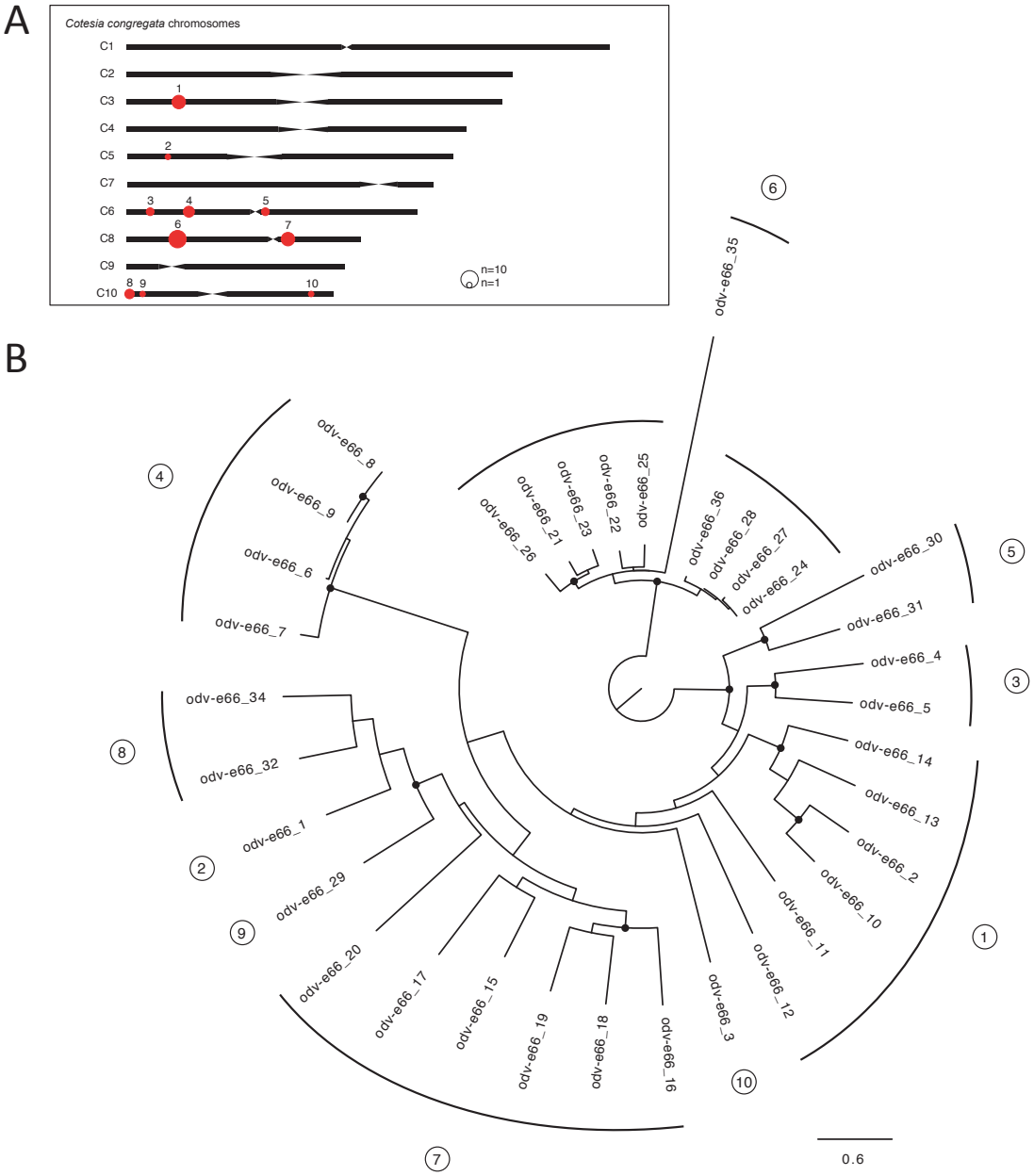

Supplementary Figure 12. Evolution of the *odv-e66* nudiviral gene family. **A.** Localization of odv-e66 genes on *C. congregata* chromosomes. The 36 *odv-e66* genes are clustered in 10 groups distributed in five different chromosomes of *C. congregata*. **B.** Maximum-likelihood phylogeny of *C. congregata* odv-e66 family (1,000 bootstraps). Prior tree construction, the regions that were present in less than 50% of the aligned sequences were manually curated from the codon-based alignment and the *odv-e66_33* gene was excluded due to its short sequence. The tree was rooted to the midpoint and the black dots indicate nodes with at least 80% of support.

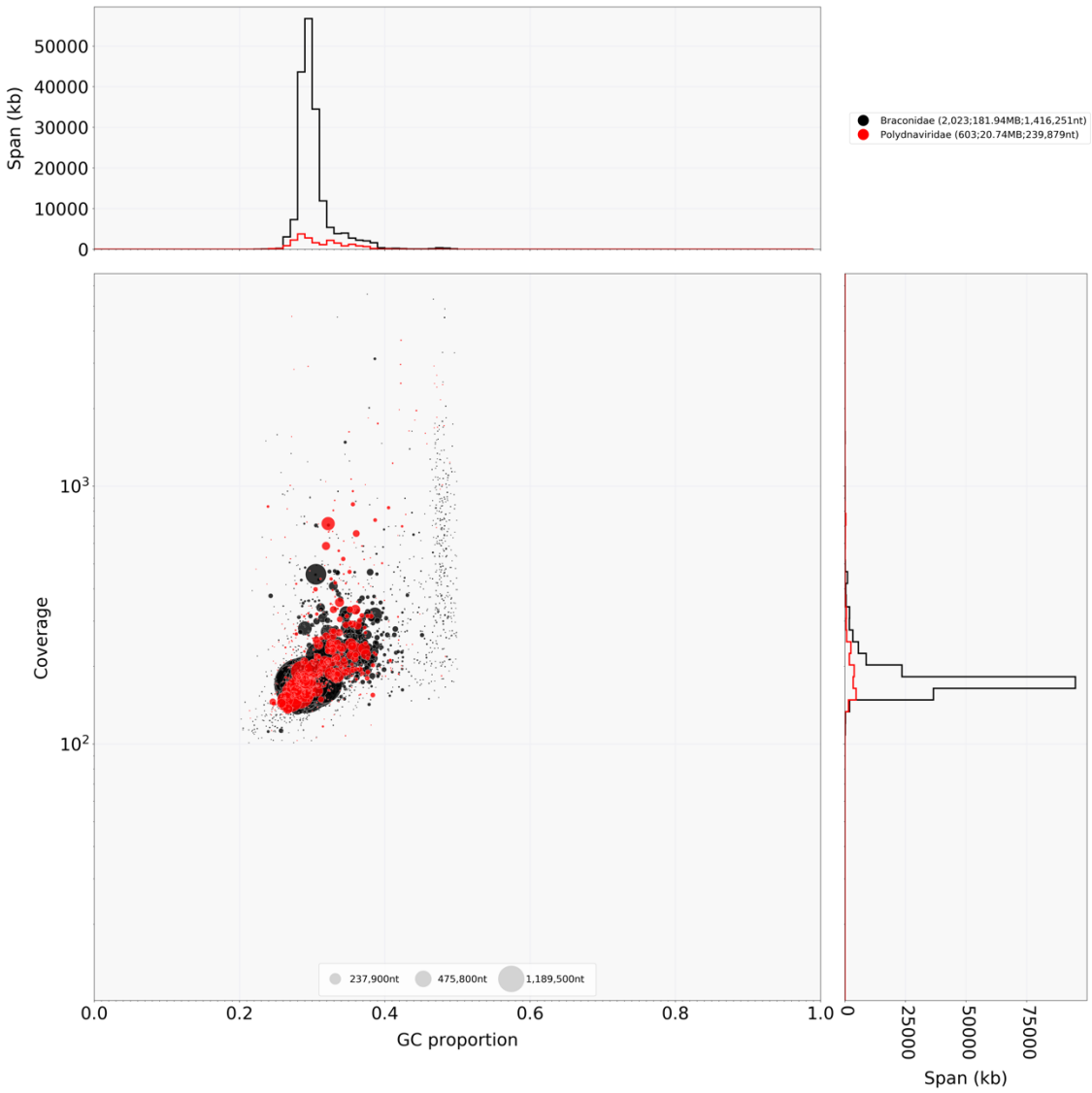

Supplementary Figure 13. Blob-plot or taxon-annotated GC content-coverage plot of *C. congregata* scaffolds. Each circle represents a scaffold in the assembly, scaled by length, and colored by order-level NCBI taxonomy assigned by BlobTools. The X axis corresponds to the average GC content of each scaffold and the Y axis corresponds to the average coverage based on alignment of Illumina reads. Marginal histograms show cumulative genome content (in Kb) for bins of coverage (Y axis) and GC content (X axis).

Supplementary Table 8. Evolutionary rates of nudiviral genes in *Cotesia* species (*C.c = C. congregata*; *C.r = C. rubecula*; *C.g = C. glomerata*; *C.v = C. vestalis*; *C.f = C. flavipes*; *C.s = C. sesamiae*; *M.d = M. demolitor.*

Protein fonction	Gene name	Gene content by species							dN/dS value	p-value
		C.c	*C. r*	*C. g*	*C. v*	*C. f*	*C. s*	*M. d*		
Replication, DNA processing	*helicase*	+	+	+	+	+	+	+	0.1343	< 0.001
	int_1	+	+	+	+	+	+	+	0.15141	< 0.001
	int_2	+	+	+	+	+	+	+	0.13921	< 0.001
	fen-1-1a	+	2	+	-	-	-	-	0.75876	0.284
	fen-1-1b	+	+	-	-	-	-	-	n.c.	n.c.
	fen-1-2	+	+	+	+	+	+	+	0.27467	< 0.001
	fen-1-3a	+	+	+	+	+	+	-	0.13039	< 0.001
	fen-1-3b	+	+	+	-	-	-	-	0.87961	0.555
	fen-1-3c	+	+	+	-	-	-	-	0.38875	< 0.001
Transcription	*p47*	+	+	+	+	+	+	+	0.05605	< 0.001
	lef-8	+	+	+	+	+	+	+	0.05973	< 0.001
	lef-9	+	+	+	+	+	+	+	0.05088	< 0.001
	lef-4	+	+	+	+	+	+	+	0.08525	< 0.001
	lef-5	+	+	+	+	+	+	+	0.36112	< 0.001
Packaging, assembly and release	*vlf-1*	+	+	+	+	+	+	+	0.17119	< 0.001
	vp91	+	+	+	+	+	+	+	0.3808	< 0.001
	vp39	+	+	+	+	+	+	+	0.72163	0.057
	p33_1	+	+	+	+	+	+	+	0.17862	< 0.001
	p33_2	2	1	1	1	1	1	1	0.15432*	< 0.001
	38K	+	+	+	+	+	+	+	0.19847	< 0.001
	p6.9_1	+	+	+	+	+	+	+	0.08337	< 0.001

	p6.9_2	+	+	+	+	+	+	+	0.70662	0.267
per os infectivity factors and ODV envelope particle components	*p74*	+	+	+	+	+	+	+	0.79274	0.058
	pif-1	+	+	+	+	+	+	+	0.45494	< 0.001
	pif-2	+	+	+	+	+	+	+	0.319	< 0.001
	pif-3	+	+	+	+	+	+	+	0.71855	0.098
	pif-4	+	+	+	+	+	+	+	0.45842	< 0.001
	pif-5_1	+	+	+	+	+	+	+	1.10226	0.38
	pif-5_2	2	1	1	1	1	1	3	0.3709*	< 0.001
	pif-6	+	+	+	+	+	+	+	0.41774	< 0.01
	HzNVorf9_1	+	+	+	+	+	+	+	0.08198	< 0.001
	HzNVorf9_2	+	+	+	+	+	+	+	0.08558	< 0.001
	GbNVorf19	+	+	+	+	+	+	+	0.30979	< 0.001
	HzNVorf64	4	1	1	1	1	1	1	0.09716*	< 0.001
	HzNVorf94	+	+	+	+	+	+	+	0.11672	< 0.001
	HzNVorf106	+	+	+	+	+	+	+	0.08689	< 0.001
	PmV	+	+	+	+	+	+	+	0.11206	< 0.001
	11K	+	+	+	+	+	+	+	0.29473	< 0.001
	HzNVorf128	+	+	+	+	+	+	+	0.11851	< 0.001
	HzNVorf140_1	3	1	1	1	1	1	1	0.19362*	< 0.001
	HzNVorf140_2	+	+	+	+	+	+	+	0.1557	< 0.001
	PmNVorf87	+	+	+	+	+	+	+	0.34099	< 0.001
	ToNVorf54_1	+	+	+	+	+	+	+	0.245	< 0.001
	ToNVorf54_2	+	+	+	+	+	+	+	0.23574	< 0.001
Other particle components	*17a_1*	+	+	+	+	+	+	+	0.96093	0.839
	17a_2	+	+	+	+	+	+	-	0.62831	< 0.05
	17b	+	+	+	+	+	+	+	0.11694	< 0.001
	27a	+	+	+	+	+	+	+	0.2348	< 0.001
	27b	+	+	+	+	+	+	+	0.24099	< 0.001

	30b	+	+	+	+	+	+	+	0.46248	< 0.001
	35a_1	+	+	+	+	+	+	+	0.74071	0.088
	35a_2	+	+	+	+	+	+	+	0.55692	< 0.001
	58b	+	+	+	+	+	+	+	0.58867	< 0.001
Unknown	*K425_438*	+	+	+	+	+	+	+	0.66340	0.076
	K425_445	+	+	+	+	+	+	+	0.83681	0.45
	K425_456	+	+	+	+	+	+	+	0.14541	< 0.001
	K425_459	+	+	+	+	+	+	+	0.20317	< 0.001
	K425_461	+	+	+	+	+	+	+	0.14772	< 0.001
	ToNVorf29	+	+	+	+	+	+	+	0.15643	< 0.001
	HzNVorf93	+	+	+	+	+	+	+	0.18237	< 0.001
	OrNVorf18	+	+	+	+	+	+	+	0.36808	< 0.001
odv-e66	*odv-e66-1*	+	+	+	+	+	+	-	0.57915	< 0.001
	odv-e66-2	+	+	+	+	+	+	+	0.84754	< 0.001
	odv-e66-3	+	+	+	+	+	+	+	0.51583	< 0.01
	odv-e66-4	+	+	+	+	+	+	-	0.53930	< 0.001
	odv-e66-5	+	+	+	+	+	+	-	0.71140	< 0.05
	odv-e66-6/7/8/9	4	1	1	3	1	1	2	n.c.	n.c.
	odv-e66-10	+	+	-	+	+	+	-	1.10867	0.589
	odv-e66-11	+	+	+	+	+	+	-	0.25798	< 0.001
	odv-e66-12	+	+	+	+	+	+	-	0.23769	< 0.001
	odv-e66-13	+	+	+	+	+	+	+	0.87336	0.439
	odv-e66-14	+	+	+	+	+	+	+	0.61298	< 0.01
	odv-e66-15	+	+	+	+	+	+	+	0.25491	< 0.001
	odv-e66-16	+	+	+	+	+	+	+	0.51120	< 0.001
	odv-e66-17	+	+	+	+	+	+	+	0.58245	< 0.001
	odv-e66-18	+	+	+	+	+	+	-	0.41734	< 0.001

	odv-e66-19	+	+	+	+	+	+	+	0.49926	< 0.001
	odv-e66-20	+	+	+	+	+	+	+	0.17390	< 0.001
	odv-e66-21/22/23/ 24/25/26/27/28	8	1	-	-	-	-	-	n.c.	n.c.
	odv-e66-29	+	+	+	+	+	+	2	0.36489	< 0.001
	odv-e66-30	+	+	+	+	+	+	-	0.85965	0.211
	odv-e66-31	+	+	-	-	-	-	-	n.c.	n.c.
	odv-e66-32	+	+	-	+	+	+	-	0.52025	< 0.001
	odv-e66-33	+	+	-	-	-	-	-	n.c.	n.c.
	odv-e66-34	+	+	-	-	-	-	-	n.c.	n.c.
	odv-e66-35	+	-	-	-	-	-	-	n.c.	n.c.
	odv-e66-36	+	-	-	-	-	-	-	n.c.	n.c.

* the closest orthologue among *C.congregata* duplications was used to estimate dN/dS
n.c. – dN/dS was not etimated when orthologues and paralogues were not distinguishable

D. Immunity

Supplementary Table 9. Immunity gene repertoires of Hymenoptera. The table indicates the number of genes annotated (including incomplete genes and pseudogenes) in six hymenopteran species.

Gene function	Pathway	Gene	Hymenoptera			Diptera	Lepidoptera	Hemiptera
			C. congregata	*N. vitripenis*	*A. mellifera*	*D. melanogaster*	*M. sexta*	*A. pisum*
Recognition		PGRP	6	11	4	13	14	0
		GNBP/βGBP	2	3	2	3	5	2
		C type lectin	2	28	12	34	34	5
		Hemolectin	1	0	1	1	2	0
		Galectin	3	3	2	6	4	2
		TEP	3	3	4	6	3	2
		Dscam	5	1	1	1	1	5
		Integrin	7	0	0	2	4	7
Signal transduction		Serine protease	58	55	57	12	107	36
		CLIP serine protease	8	28	18	45	54	3
		Serpins	4	12	7	29	34	14
	Toll	Spätzle	3	6	2	6	8	10
		Toll receptor	7	6	5	9	16	7
		MyD88	1	1	1	1	1	1
		Tube	2	1	1	1	1	1
		Pelle	2	1	1	1	1	1

Signalling pathways	IMD/JNK	ANK/Cactus	1	1	3	1	1	1
		Dif/Dorsal	1	2	2	2	5	2
		IMD	1	1	1	1	1	0
		FADD	1	n.d.	1	1	1	1
		Dredd_IMD	1	1	1	1	1	0
		Tab2_IMD	1	1	2	1	1	1
		IAP2	5	n.d.	1	1	1	1
		ird5-IKKg	1	1	1	1	1	1
		TAK1_IMD	1	n.d.	1	1	1	1
		IKKg (Kenny)	0	1	1	1	1	0
		Bendless-Ubc13	1	n.d.	1	1	1	1
		Relish_IMD	1	3	1	1	1	0
		JNK kinase (Hemipterous-MKK7)	1	n.d.	1	3	1	1
		Basket-JNK	1	1	1	1	1	1
		Fos - kayak transcription factor	1	1	1	1	1	0
		c-Jun	1	n.d.	1	1	1	1
	JAK/STAT	Upd3	0	n.d.	0	1	0	0
		PIAS	3	1	3	1	1	n.d.
		SOCS	1	n.d.	2	1	1	3
		Domeless	1	1	1	1	1	3
		Hopscotch (JAK)	1	1	4	1	1	1
		STAT	1	n.d.	1	1	1	2
	Melanization	Pro Phenol Oxidase	1	3	1	3	2	2
	Anti-microbial peptides	Hymenoptaecin	1	1	1	0	0	0
		Moricin	0	0	0	0	6	0
		Lebocin	0	0	0	0	4	0
		Defensin	6	2	2	1	24	0

Effectors		Lysozyme	1	1	3	13	6	3
		Chitinase	11	4	5	16	11	7
		Transferrin	3	2	1	2	4	2
		Peroxidase	14	15	13	20	3	15
	Others	Nitric Oxide Synthase (NOS)	1	1	1	1	2	1
		Super Oxide Dismutase	4	4	2	4	4	4
		Glutathione S Transferase	8	7	5	35	31	18
		MIF	0	0	0	0	1	5
		Heat Shock Protein	11	4	4	13	16	15
Antiviral immuniy	RNAi pathways	Dicer 1	1	0	1	1	1	1
		Dicer 2	1	0	1	1	1	1
		Argonaute	3	0	1	3	1	4
		R2D2	1	0	1	1	1	1
		Vago	0	0	1	1	1	0

n.d. for not determined

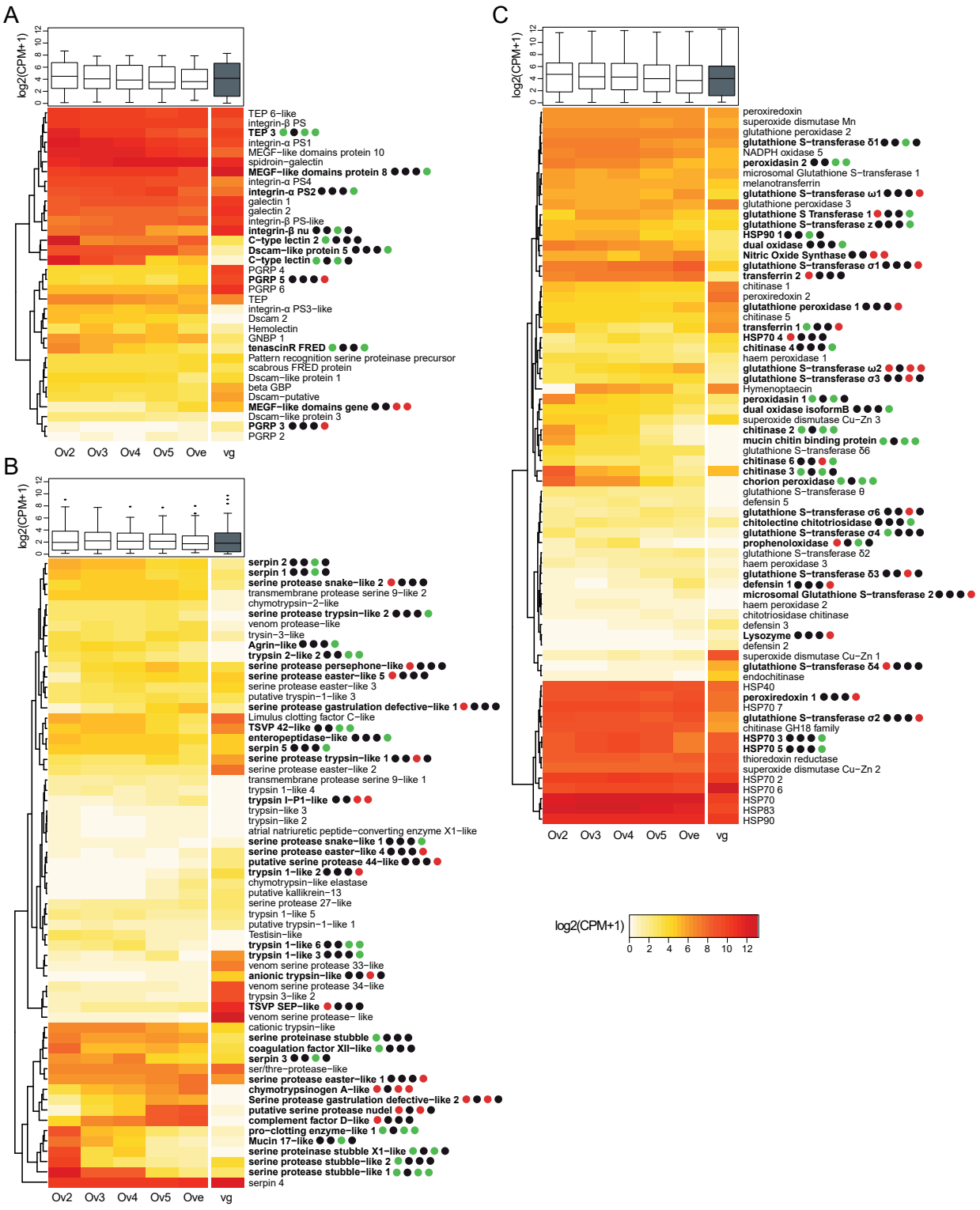

Supplementary Figure 14. Gene expression of immunity genes during *Cotesia congregata* development. Heatmaps show the expression of the genes involved in **A** signal recognition, **B** signal transduction and **C** effector functions across the developmental stages of ovaries (Ov2, Ov3, Ov4, Ov5, Ove) and in venom glands (vg). The trees on the left are unsupervised hierarchical

clustering of expression values. Boxplots represent overall expression of each immunity gene group in ovaries and venom glands. Bold names highlight the genes that are differentially expressed and dots represent the four different comparisons studied between consecutive ovary stages (Ov2 *vs.* Ov3, Ov3 *vs*. Ov4, Ov4 *vs*. Ov5 and Ov5 *vs.* Ove). Black, red and green dots indicate similar, increased and reduced expressions between consecutive developmental stages respectively.

E. Chemoreceptor

To find their hosts, female wasps follow scents emitted by caterpillars and the plants they damage. The host identification process for oviposition acceptance occurs mainly during contact between the parasitoid and its host, when host products related to feeding activities, fecal pellets and oral secretions, play a crucial role. In insects, chemical signals are detected by sensory neurons expressing transmembrane receptor genes belonging to three different families: the odorant receptors (ORs) that are devoted to olfaction, the gustatory receptors (GRs) which are involved in taste, and the ionotropic receptors (IRs) that include receptors used in both chemosensory modalities[18]. We annotated these chemoreceptor gene families in the genome of *C. congregata*, and identified genes encoding 243 ORs and 54 GRs. These numbers are in the range of those obtained for other parasitoid wasps, either within the family Braconidae or in *N. vitripennis*, but remain lower than in ants (Supplementary Table 10). We also identified 105 IRs, whereas only 56 have been annotated in *Diachasma alloeum*, another Braconidae.

Focusing on ORs, we performed expert annotation and manual curation, resulting in 197 full-length gene sequences (encoding >350 amino acids) and 46 incomplete genes. A phylogenetic analysis of ORs from *C. congregata* and four other Hymenoptera species (*M. demolitor*, *N. vitripennis*, *A. mellifera*) showed that *C. congregata* ORs belong to 15 of the 18 strongly supported monophyletic OR lineages (aLRT ≥ 0.9) (Fig. 2), which have been previously described in Apocrita[30]. Using this phylogeny, we analyzed the dynamics of OR gene gains and losses and found that the equally high number of OR genes in *N. vitripennis* and in Braconidae (*M. demolitor* and *C. congregata*) results from independent expansions (Supplementary Fig.14). The number of OR genes in the last common ancestor of these parasitoid wasps may have been rather low (~60), and many duplication events occurred after the split between Braconidae and other parasitoid wasps. The most spectacular Braconidae-specific expansions occurred in clades B, C/D/E, F, Q/R/S and 9-exon, each harboring at least 25 genes in *C. congregata* (Fig 2; Supplementary Table 11). As expected, highly duplicated OR genes in *C. congregata* were found in 6 clusters of at least 10 tandemly arrayed genes, the largest one containing 19 genes (Supplementary Fig. 15). Even within Braconidae, many duplications occurred in ancestors of *Cotesia* species after the split with the lineage of *M. demolitor* (Fig. 2). We also identified Braconidae-specific gene losses, notably in subfamilies A, V and Z. This illustrates how dynamic is the evolution of OR genes within parasitoid wasps.

In an attempt to study whether different host specificities of *Cotesia* species could be linked with differences in OR repertoires, we annotated OR genes in four other *Cotesia* species. *C. congregata*, *C. sesamiae* and *C. flavipes* are parasitizing a large range of lepidopteran species, whereas *C. rubecula* and *C. vestalis* are specialists on *Pieris rapae* and *Plutella xylostella* larvae, respectively. Interestingly, OR copy numbers varied significantly during the evolution of the genus *Cotesia*, and higher numbers of OR genes were found in the two specialist species (Supplementary Table 11). The lack of phylogenetic resolution for closely related *Cotesia* OR genes precluded any comprehensive analysis of gene gains and losses, but we found several expansions in *C. rubecula* and *C. vestalis* within many OR clades (Supplementary Fig. 16).

Supplementary Table 10. Chemoreceptor gene repertoires of Hymenoptera. The table indicates the number of OR, GR and IR genes annotated (including incomplete genes and pseudogenes) in seven hymenopteran species.

	Braconidae			Pteromalidae	Formicidae	Apidae	Cephidae
Species	*C. congregata*	*M. demolitor*	*D. alloeum*	*N. vitripennis*	*P. barbatus*	*A. mellifera*	*C. cinctus*
ORs	243	203	201	216	399	162	73
GRs	54	86	40	58	73	13	35
IRs	105	n.d.	56	153	24	21	49
Citation	This study	26	27	28 29 30	31 30	27 28 30 32	28

n.d. for not determined

Supplementary Table 11. OR copy number per subfamily[26] compared to data obtained from genomes of *Cotesia* species.

OR subfamily	*C. congregata*	*C. rubecula*	*C. vestalis*	*C. flavipes*	*C. sesamiae*	*M. demolitor*	*N. vitripennis*	*A. mellifera*	*C. cinctus*
A	0	0	0	0	0	0	0	3	1
B	34	42	33	28	29	27	0	1	1
CDE	34	42	39	33	28	36	34	7	14
F	28	25	28	22	23	20	20	1	0
GHX	21	22	19	15	17	16	12	16	1
J	1	1	1	1	1	3	0	19	12
KL	16	20	12	9	9	14	8	59	8
MNOP	12	18	13	10	12	8	3	6	0
QRS	25	34	23	15	16	21	4	1	11
TU	11	10	12	9	9	12	22	3	4
V	0	0	0	0	0	0	9	6	1
Z	0	0	0	0	0	0	13	1	2
ZB	14	24	19	17	11	10	19	0	1
9-exon	34	45	40	32	31	31	61	34	2
Other	13	13	13	11	11	5	11	5	15
Total	243	296	252	202	197	203	216	162	73

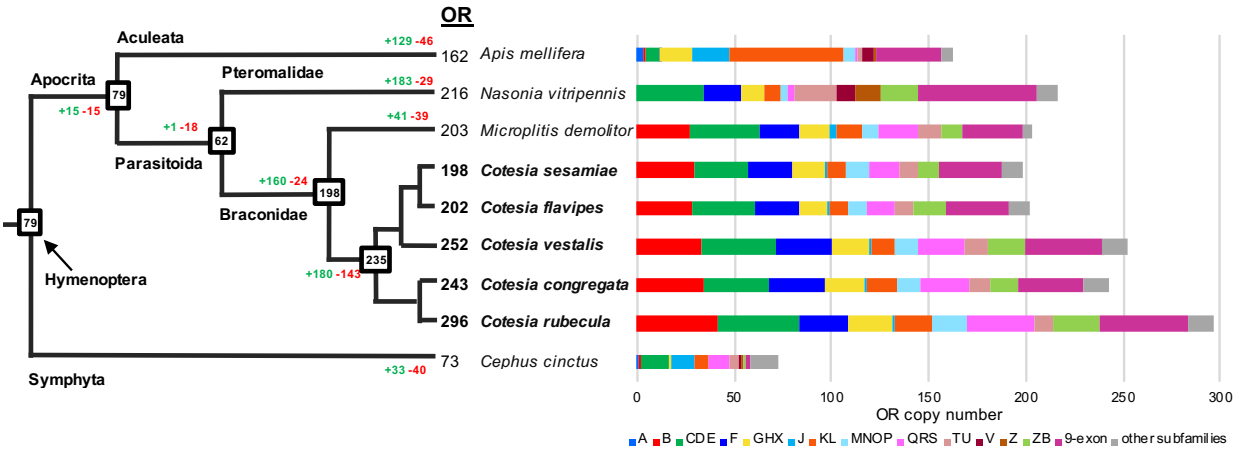

Supplementary Figure 15. Copy number dynamics of OR genes in five Cotesia species and four other Hymenoptera species. Estimated numbers of gene gain and loss events are shown on each branch of the species tree in green and red, respectively. The size of OR repertoires in common ancestors is indicated in boxes at the corresponding nodes of the species tree. The histogram represents the distribution of OR copy number per subfamily for each species.

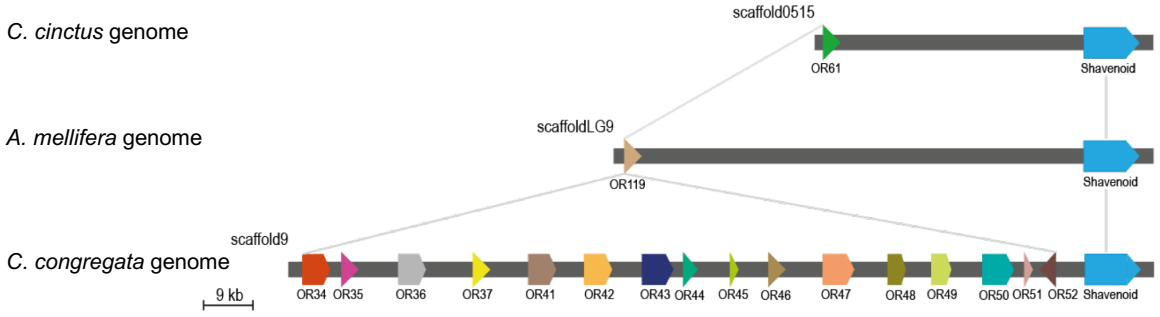

Supplementary Figure 16. Synteny among the OR subfamily B in *C. congregata*, *C. cinctus* and *A. mellifera*, based on inter-specific conservation of the shavenoid gene, showing expansion through tandem duplications for *C. congregate* OR genes. Orientation (arrows) of genes within scaffolds are indicated.

A

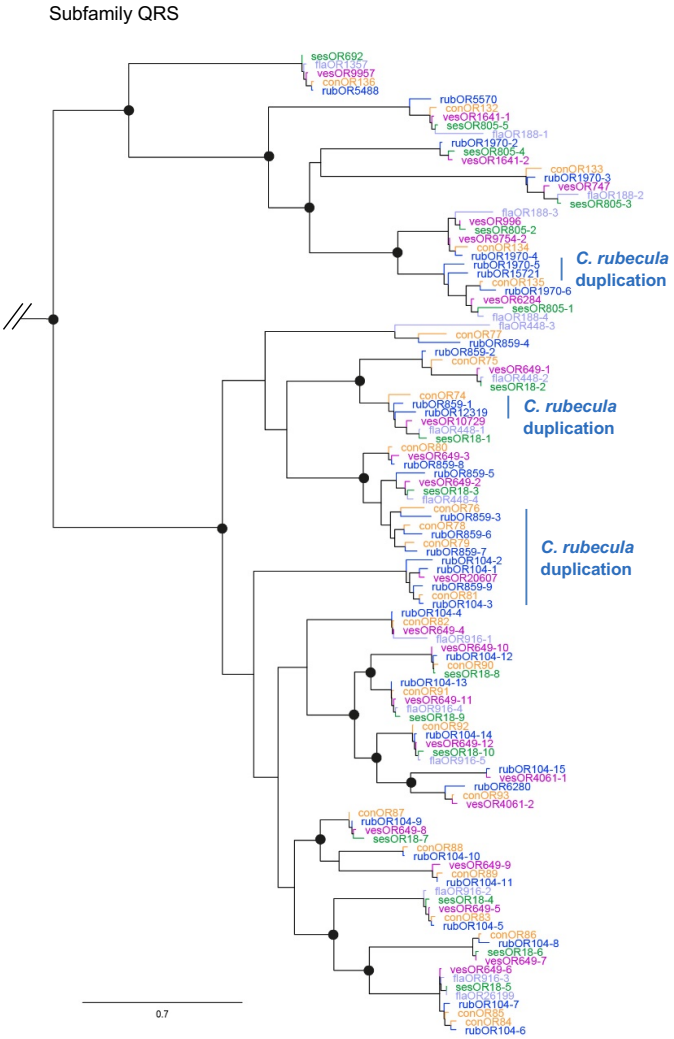
Subfamily QRS
sesOR692
flaOR1957
vesOR9957
conOR138
rubOR5488
rubOR5570
conOR132
vesOR1641-1
sesOR805-5
flaOR188-1
rubOR1970-2
sesOR805-4
vesOR1641-2
conOR133
rubOR1970-3
vesOR747
flaOR188-2
sesOR805-3
flaOR188-3
vesOR996
sesOR805-2
vesOR9754-2
conOR134
rubOR1970-4
rubOR1970-5
rubOR15721
C. rubecula duplication
conOR135
rubOR1970-6
vesOR6284
sesOR805-1
flaOR188-4
flaOR448-3
conOR77
rubOR859-4
rubOR859-2
conOR75
vesOR649-1
flaOR448-2
sesOR18-2
conOR74
rubOR859-1
rubOR12319
vesOR10729
flaOR448-1
sesOR18-1
C. rubecula duplication
conOR80
vesOR649-3
rubOR859-8
rubOR859-5
vesOR649-2
sesOR18-3
flaOR448-4
conOR76
rubOR859-3
conOR79
rubOR859-6
conOR78
rubOR859-7
rubOR104-2
rubOR104-1
vesOR20607
rubOR859-9
conOR81
rubOR104-3
C. rubecula duplication
rubOR104-4
conOR82
vesOR649-4
flaOR916-1
vesOR649-10
rubOR104-12
conOR90
sesOR18-8
rubOR104-13
conOR91
vesOR649-11
flaOR916-4
sesOR18-9
conOR92
rubOR104-14
vesOR649-12
sesOR18-10
flaOR916-5
rubOR104-15
vesOR4061-1
rubOR6280
conOR93
vesOR4061-2
conOR87
rubOR104-9
vesOR649-8
sesOR18-7
conOR88
rubOR104-10
vesOR649-9
conOR89
rubOR104-11
flaOR916-2
sesOR18-4
vesOR649-5
conOR83
rubOR104-5
conOR86
rubOR104-8
sesOR18-6
vesOR649-7
vesOR649-6
flaOR916-3
sesOR18-5
flaOR24199
rubOR104-7
conOR85
conOR84
rubOR104-6
0.7

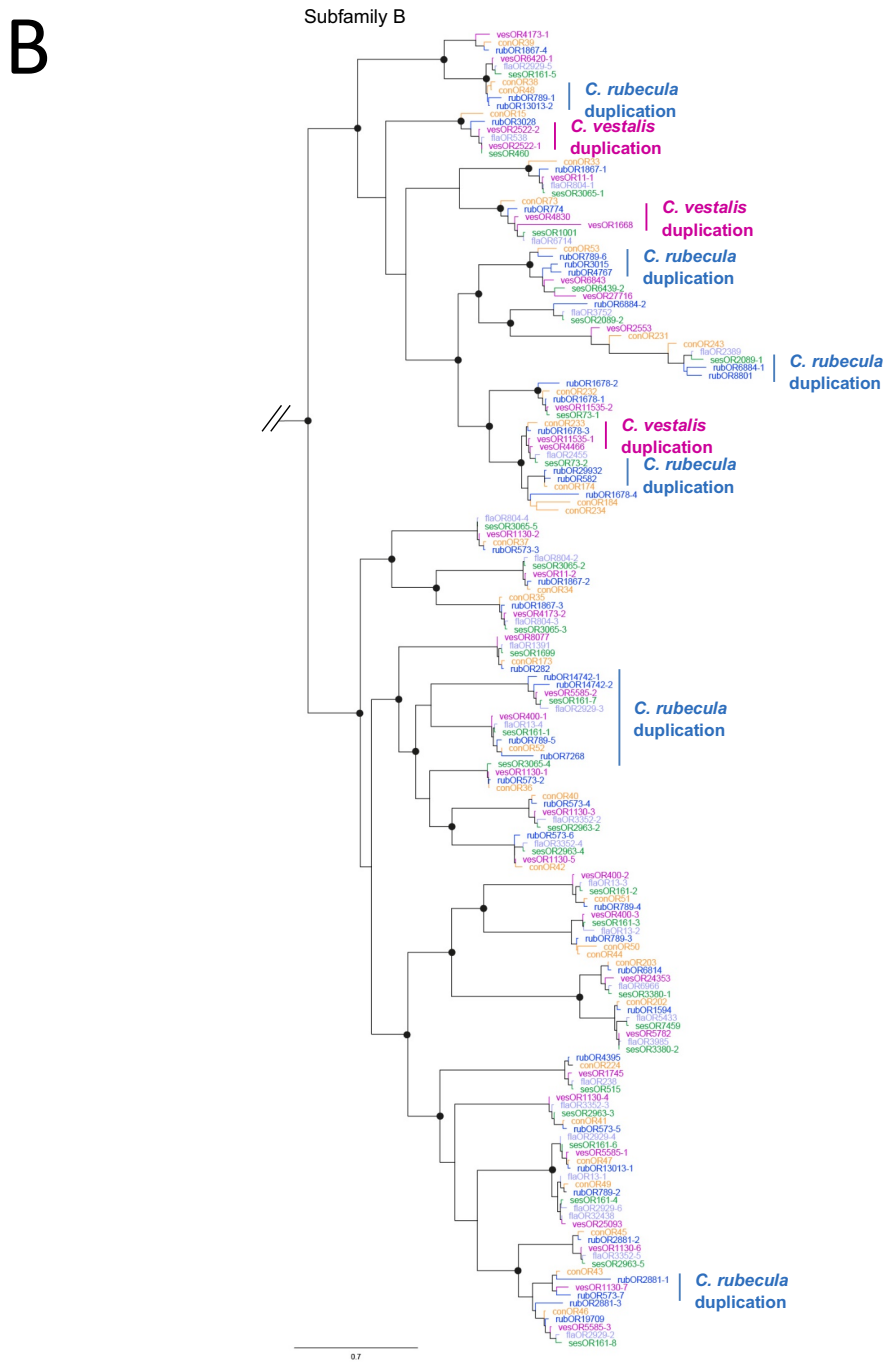

Supplementary Figure 17. Phylogenies of OR subfamilies **A** QRS and **B** B in five *Cotesia* species. These subtrees were extracted from maximum-likelihood phylogeny of *Cotesia* ORs including OR repertoires from *C. congregata* (con, orange), *C. flavipes* (fla, purple), *C. rubecula* (rub, blue), *C. sesamiae* (ses, green) and *C. vestalis* (ves, pink). The tree was rooted using the Orco clade as outgroup. Circles indicate nodes strongly supported by the approximate likelihood-ratio test (aLRT ≥ 0.95). The scale bar represents 0.7 expected amino acid substitutions per site. *C. rubecula* and *C. vestalis* duplications are highlighted on the right.

F. Detoxification

Supplementary Table 12. Detoxification gene repertoires of Hymenoptera. The table indicates the number of genes annotated (including incomplete genes and pseudogenes) in six hymenopteran species.

	Hymenoptera			Diptera	Lepidoptera	Hemiptera
Enzyme family	*C. congregata*	*N. vitripennis*	*A. mellifera*	*D. melanogaster*	*M. sexta*	*A. pisum*
P450	70	87	46	86	103	64
CCE	35	41	24	35	96	30
GST	17	19	10	40	31	20
UGT	11	22	12	34	43	57
ABC	46	55	41	56	53	70
Citation	This study	[33]	[34, 35]	[36, 37]	[38, 39]	[40]

Supplementary Table 13. Detoxification gene repertoires of *Cotesia* species. The table indicates the number of genes annotated (including incomplete genes and pseudogenes) in six *Cotesia* species.

Enzyme family	*C. congregata*	*C. rubecula*	*C. glomerata*	*C. vestalis*	*C. flavipes*	*C. sesamiae*
P450	70	68	70	65	48	50
CCE	26	32	30	27	22	24
GST	17	18	n.d.	17	17	17
UGT	10	10	n.d.	10	10	10
ABC	46	49	47	46	44	44

n.d. for not determined

Supplementary Table 14. Detailled detoxification gene repertoires of *Cotesia* species. The table indicates the number of genes annotated (including incomplete genes and pseudogenes) in six *Cotesia* species.

		C. congregata	*C. rubecula*	*C. glomerata*	*C. vestalis*	*C. flavipes*	*C. sesamiae*
P450	CYP2 clan	10	9	n.d.	9	9	9
	CYP3 clan	36	33	n.d.	31	25	24
	CYP4 clan	18	15	n.d.	14	9	10
	mito clan	6	6	n.d.	6	6	6
CCE	Clade A	14	16	12	14	12	13
	Clade B	5	8	10	8	5	6
	Clade D	1	2	2	1	1	1
	Clade E	4	4	4	2	2	2
	Clade F	2	2	2	2	2	2
GST	Delta	5	7	n.d.	6	6	6
	Epsilon	0	0	n.d.	0	0	0
	Omega	2	2	n.d.	2	2	2
	Sigma	5	5	n.d.	5	5	5
	Theta	1	1	n.d.	1	1	1
	Zeta	1	1	n.d.	1	1	1
	microsomal	2	16	n.d.	15	15	15
	unclassified	2	2	n.d.	2	2	2
UGT	classe 1	0	0	n.d.	0	0	0
	classe 2	1	1	n.d.	1	1	1
	classe 3	0	0	n.d.	0	0	0
	classe 4a	4	4	n.d.	4	4	4
	classe 4b	1	1	n.d.	1	1	1
	classe 4c	2	2	n.d.	2	2	2
	classe 5	1	1	n.d.	1	1	1
	classe 6	1	1	n.d.	1	1	1
	unclassified	0	0	n.d.	0	0	0
ABC	subfamily A	4	4	4	4	4	4
	subfamily B	4	4	3	3	3	3
	subfamily C	16	17	17	14	16	16
	subfamily D	2	2	2	2	2	2
	subfamily E	1	2	1	2	1	0
	subfamily F	3	4	3	4	3	3

	subfamily G	13	13	14	14	12	13
	subfamily H	3	3	3	3	3	3

n.d. for not determined

Supplementary References

1. Belle, E. *et al.* Visualization of polydnavirus sequences in a parasitoid wasp chromosome. *J Virol* **76**, 5793-6 (2002).
2. Bao, W., Jurka, M.G., Kapitonov, V.V. & Jurka, J. New superfamilies of eukaryotic DNA transposons and their internal divisions. *Mol Biol Evol* **26**, 983-93 (2009).
3. Warburton, P.E., Giordano, J., Cheung, F., Gelfand, Y. & Benson, G. Inverted repeat structure of the human genome: the X-chromosome contains a preponderance of large, highly homologous inverted repeats that contain testes genes. *Genome Res* **14**, 1861-9 (2004).
4. Edgar, R.C. Search and clustering orders of magnitude faster than BLAST. *Bioinformatics* **26**, 2460-1 (2010).
5. Katoh, K. & Standley, D.M. MAFFT multiple sequence alignment software version 7: improvements in performance and usability. *Mol Biol Evol* **30**, 772-80 (2013).
6. Price, M.N., Dehal, P.S. & Arkin, A.P. FastTree: computing large minimum evolution trees with profiles instead of a distance matrix. *Mol Biol Evol* **26**, 1641-50 (2009).
7. Peters, R.S. *et al.* Evolutionary History of the Hymenoptera. *Curr Biol* **27**, 1013-1018 (2017).
8. Kawahara, A.Y. & Breinholt, J.W. Phylogenomics provides strong evidence for relationships of butterflies and moths. *Proc Biol Sci* **281**, 20140970 (2014).
9. Gasmi, L. *et al.* Recurrent Domestication by Lepidoptera of Genes from Their Parasites Mediated by Bracoviruses. *PLoS Genet* **11**, e1005470 (2015).
10. Bézier, A. *et al.* Polydnaviruses of braconid wasps derive from an ancestral nudivirus. *Science* **323**, 926-30 (2009).
11. Kittel, R.N., Austin, A.D. & Klopfstein, S. Molecular and morphological phylogenetics of chelonine parasitoid wasps (Hymenoptera: Braconidae), with a critical assessment of divergence time estimations. *Mol Phylogenet Evol* **101**, 224-241 (2016).
12. Shimbori, E.M. *et al.* Revision of the New World genera Adelius Haliday and Paradelius de Saeger (Hymenoptera: Braconidae: Cheloninae: Adeliini). *Zootaxa* **4571**, 151-200 (2019).
13. Sharkey, M., van Noort, S. & Whitfield, J.B. Revision of Khoikhoiine (Hymenoptera, Braconidae). . *ZooKeys* **20**, 299-348. (2009).
14. Whitfield, J.B. & Mason, W.R.M. Mendesellinae, a new subfamily of braconid wasps (Hymenoptera, Braconidae) with a review of relationships within the microgastroid assemblage. *Systematic Entomology* **19**, 61-76 (1994).

15. Quicke, D.L.J. & Van Achterberg, C. Phylogeny of the subfamilies of the family Braconidae (Hymenoptera: Ichneumonoidea). *Zoologishe Verhandelingen* **258**, 1-95 (1990).
16. Whitfield, J.B. Molecular and morphological data suggest a single origin of the polydnaviruses among braconid wasps. *Naturwissenschaften* **84**, 502-507 (1997).
17. Dowton, M. & Austin, A.D. Phylogenetic relationships among the microgastroid (Hymenoptera : Braconidae) : combined analysis of 16S and 28S rDNA genes, and morphological data. *Mol. Phyl. Evol.* **10**, 354-366 (1998).
18. Whitfield, J.B., Mardulyn, P., Austin, A.D. & Dowton, M. Phylogenetic relationships among microgastrine braconid wasp genera based on data from the 16S, COI and 28S genes and morphology. *Systematic Entomology* **27**, 337-359 (2002).
19. Whitfield, J.B. & Lockhart, P.J. Deciphering ancient rapid radiations. *Trends Ecol Evol* **22**, 258-65 (2007).
20. Murphy, N., Banks, J.C., Whitfield, J.B. & Austin, A.D. Phylogeny of the parasitic microgastroid subfamilies (Hymenoptera: Braconidae) based on sequence data from seven genes, with an improved time estimate of the origin of the lineage. *Mol. Phylogenet. Evol.* **47**, 378-95 (2008).
21. Sharanowski, B.J., Dowling, A.P.G. & J., S.M. Molecular phylogenetics of Braconidae (Hymenoptera: Ichneumonoidea), based on multiple nuclear genes, and implications for classification. *Systematic Entomology* **36**, 549-572 (2011).
22. Thézé, J., Bézier, A., Periquet, G., Drezen, J.M. & Herniou, E.A. Paleozoic origin of insect large dsDNA viruses. *Proc Natl Acad Sci U S A* **108**, 15931-5 (2011).
23. Fernandez-Triana, J.L. & Boudreault, C. Seventeen new genera of microgastrine parasitoid wasps (Hymenoptera, Braconidae) from tropical areas of the world. *Journal of hymenoptera research* **64**, 25-140 (2018).
24. Mardulyn, P. & Whitfield, J.B. Phylogenetic signal in the COI, 16S, and 28S genes for inferring relationships among genera of Microgastrinae (Hymenoptera; Braconidae): Evidence of a high diversification rate in this group of parasitoids. *Molecular Phylogenetics and Evolution* **12**, 282-294 (1999).
25. Banks, J.C. & Whitfield, J.B. Dissecting the ancient rapid radiation of microgastrine wasp genera using additional nuclear genes. *Mol Phylogenet Evol* **41**, 690-703 (2006).
26. Zhou, X. *et al.* Chemoreceptor Evolution in Hymenoptera and Its Implications for the Evolution of Eusociality. *Genome Biol Evol* **7**, 2407-16 (2015).
27. Tvedte, E.S. *et al.* Genome of the Parasitoid Wasp Diachasma alloeum, an Emerging Model for Ecological Speciation and Transitions to Asexual Reproduction. *Genome Biol Evol* **11**, 2767-2773 (2019).
28. Robertson, H.M. Molecular Evolution of the Major Arthropod Chemoreceptor Gene Families. . *Annual Review of Entomology* **64**, 227-242 (2019).
29. Robertson, H.M., Gadau, J. & Wanner, K.W. The insect chemoreceptor superfamily of the parasitoid jewel wasp Nasonia vitripennis. *Insect Mol Biol* **19 Suppl 1**, 121-36 (2010).
30. Zhou, X. *et al.* Phylogenetic and transcriptomic analysis of chemosensory receptors in a pair of divergent ant species reveals sex-specific signatures of odor coding. *PLoS Genet* **8**, e1002930 (2012).
31. Smith, C.R. *et al.* Draft genome of the red harvester ant Pogonomyrmex barbatus. *Proc Natl Acad Sci U S A* **108**, 5667-72 (2011).

32. Croset, V. *et al.* Ancient protostome origin of chemosensory ionotropic glutamate receptors and the evolution of insect taste and olfaction. *PLoS Genet* **6**, e1001064 (2010).
33. Oakeshott, J.G. *et al.* Metabolic enzymes associated with xenobiotic and chemosensory responses in Nasonia vitripennis. *Insect Mol Biol* **19 Suppl 1**, 147-63 (2010).
34. Claudianos, C. *et al.* A deficit of detoxification enzymes: pesticide sensitivity and environmental response in the honeybee. *Insect Mol Biol* **15**, 615-36 (2006).
35. Liu, S. *et al.* Genome-wide identification and characterization of ATP-binding cassette transporters in the silkworm, Bombyx mori. *BMC Genomics* **12**, 491 (2011).
36. Adams, M.D. *et al.* The genome sequence of *Drosophila melanogaster*. *Science* **287**, 2185-95 (2000).
37. Tijet, N., Helvig, C. & Feyereisen, R. The cytochrome P450 gene superfamily in Drosophila melanogaster: Annotation, intron-exon organization and phylogeny. (2001).
38. Kanost, M.R. *et al.* Multifaceted biological insights from a draft genome sequence of the tobacco hornworm moth, Manduca sexta. *Insect Biochem Mol Biol* **76**, 118-147 (2016).
39. Qi, W. *et al.* Characterization and expression profiling of ATP-binding cassette transporter genes in the diamondback moth, Plutella xylostella (L.). *BMC Genomics* **17**, 760 (2016).
40. Ramsey, J.S. *et al.* Comparative analysis of detoxification enzymes in Acyrthosiphon pisum and Myzus persicae. *Insect Mol Biol* **19 Suppl 2**, 155-64 (2010).